Axonal and neuromuscular synaptic phenotypes in Wld(S), SOD1(G93A) and ostes mutant mice identified by fiber-optic confocal microendoscopy

Molecular and Cellular Neuroscience, Volume 42, Issue 4, November 2009, Pages 296–307
http://dx.doi.org/10.1016/j.mcn.2009.08.002

AXONAL AND NEUROMUSCULAR SYNAPTIC PHENOTYPES IN *Wld^S*, *SOD1^{G93A}* AND *ostes* MUTANT MICE IDENTIFIED BY FIBER-OPTIC CONFOCAL MICROENDOSCOPY

By

Frances Wong[1,2], Li Fan[1], Sara Wells[2], Robert Hartley[1], Francesca E. Mackenzie[2], Oyinlola Oyebode[1], Rosalind Brown[1], Derek Thomson[1], Michael P. Coleman[3], Gonzalo Blanco*[2] and Richard R Ribchester*[1]

**These authors contributed equally to the design and management of this study.*

Correspondence: Richard.Ribchester@ed.ac.uk

1. Euan MacDonald Centre for MND Research
The University of Edinburgh
George Square
Edinburgh
EH8 9JZ
UK

2. Mouse Neuromuscular Genetics Group
MRC Mammalian Genetics Unit
Harwell,
OX11 0RD
UK

3. Laboratory of Molecular Signalling
The Babraham Institute,
Babraham,
Cambridge
CB22 3AT

Short title: Covert neuromuscular phenotypes
Key words: neuromuscular junction; motor neuron; neurodegeneration; peripheral nerve; mouse mutant; regeneration; ALS; imaging

Molecular and Cellular Neuroscience, Volume 42, Issue 4, November 2009, Pages 296–307
http://dx.doi.org/10.1016/j.mcn.2009.08.002

ABSTRACT

We used live imaging by fiber-optic confocal microendoscopy (CME) of yellow fluorescent-protein (YFP) expression in motor neurons to observe and monitor axonal and neuromuscular synaptic phenotypes in mutant mice. First, we visualized slow degeneration of axons and motor nerve terminals at neuromuscular junctions following sciatic nerve injury in *Wld*^{S} mice with slow Wallerian degeneration. Protection of axotomised motor nerve terminals was much weaker in *Wld*^{S} heterozygotes than in homozygotes. We then induced covert modifiers of axonal and synaptic degeneration in heterozygous *Wld*^{S} mice, by N-ethyl-N-nitrosourea (ENU)-mutagenesis, and used CME to identify candidate mutants that either enhanced or suppressed axonal or synaptic degeneration. From 219 of the F1 progeny of ENU-mutagenized BALB/c mice and *thy1.2-YFP16/Wld*^{S} mice, CME revealed six phenodeviants with suppression of synaptic degeneration. Inheritance of synaptic protection was confirmed in three of these founders, with evidence of Mendelian inheritance of a dominant mutation in one of them (designated CEMOP_S5). We next applied CME repeatedly to living *Wld*^{S} mice and to SOD1^{G93A} mice, an animal model of motor neuron disease, and observed degeneration of identified neuromuscular synapses over a 1-4 day period in both of these mutant lines. Finally, we used CME to observe slow axonal regeneration in the ENU-mutant *ostes* mouse strain. The data show that CME can be used to monitor covert axonal and neuromuscular synaptic pathology and, when combined with mutagenesis, to identify genetic modifiers of its progression *in vivo.*

Molecular and Cellular Neuroscience, Volume 42, Issue 4, November 2009, Pages 296–307
http://dx.doi.org/10.1016/j.mcn.2009.08.002

INTRODUCTION

Many neurodegenerative diseases, ranging from Amyotrophic Lateral Sclerosis (ALS) to Alzheimer's Disease, remain intractable despite more than a decade of research using mutants and transgenic models in mice and other species (Bruijn and Cleveland, 1996; Bruijn et al., 2004; Gotz et al., 2007; Gotz and Ittner, 2008; Jackson et al., 2002). However, discovery of novel pathways for neuroprotection or enhancement of regeneration in animal models continues to be important for identifying new targets for treatment of disease. One approach is through genome-wide mutagenesis, a powerful methodology that has generated new animal models and provided insight into cell biological mechanisms of development and normal physiological functions.

Screening for mutations generated by N-ethyl-N-nitrosourea (ENU) in mice is one proven method for discovery of novel gene functions. For instance, mutant phenotypes identified by ENU-mutagenesis screens have led to better understanding of diseases ranging from complex behavioral dysfunctions to autoimmune disorders (for recent reviews see (Acevedo-Arozena et al., 2008; Cook et al., 2006; Godinho and Nolan, 2006; Gondo, 2008). ENU screens are required to achieve sufficient throughput to identify mutants within a relatively short overall time frame. They should also be non-invasive, or minimally-invasive, since phenodeviant founders identified in a screen are the only resource for breeding and testing of inheritance of the deviant phenotype(s). Standardized protocols such as SHIRPA (Nolan et al., 2000) readily expose overt neurological phenotypes in ENU screens. However, these methods are less suitable for identifying *covert* phenotypes that may be protective, or otherwise beneficial, and thus producing no overt neurological signs. Such phenotypes will normally be missed in primary screens that are restricted to detection of external or behavioural anomalies.

The most compelling precedent for discovery and importance of covert, neuroprotective phenotypes was the serendipitous finding of slow Wallerian degeneration in the spontaneous mutant *Wld*^{S} mouse. In these mice, orthograde degeneration of distal axons after nerve injury is delayed by 1-4 weeks (Lunn et al., 1989; Lyon et al., 1993; Perry et al., 1990b). Once this remarkable phenotype had been established, systematic molecular genetic analysis was then used to show that the mutation underlying it encodes a chimeric Ube4b-Nmnat1 protein that, when

Molecular and Cellular Neuroscience, Volume 42, Issue 4, November 2009, Pages 296–307
http://dx.doi.org/10.1016/j.mcn.2009.08.002

expressed in transgenic mice, reproduces the slow-degeneration of axons and neuromuscular synapses observed in the natural mutant (Coleman et al., 1998; Conforti et al., 2000; Mack et al., 2001). Subsequent detailed phenotypic analysis showed that axon protection in peripheral nerves of *Wld*^{S} mice following nerve section is very strong: distal axons are preserved for 21 days or more after the nerve injury (Lunn et al., 1990; Perry et al., 1990a; Perry et al., 1992; Perry et al., 1990b). The amount of axon protection also varies in a 'gene-dose' dependent fashion: that is, the number of preserved axons in a low stringency assay performed at 3 days after nerve section showed variation among transgenic mouse lines as a function of their Wld^S protein expression (Mack et al., 2001).

Interestingly, Western-blot analysis of brain and quantitative measurements of immunostaining for Wld^S protein in brain and spinal cord show expression levels in heterozygotes at about half the level in homozygotes. However, the level of axon protection in *Wld*^{S} heterozygotes is virtually the same as in homozygotes (Beirowski et al., 2005; Mack et al., 2001; Wilbrey et al., 2008). Despite this, protection of axons by the *Wld*^{S} gene in both the native mutant and in the transgenic equivalents is stronger than that of motor nerve terminals, suggesting that degeneration of motor nerve terminals may be regulated differently from axons (Gillingwater and Ribchester, 2001; Gillingwater et al., 2002). Synaptic protection further declines with age: thus, in *Wld*^{S} mice aged over about 8 months very few intact motor nerve terminals are present by 3 days after nerve injury (Gillingwater et al., 2002; Perry et al., 1992; Ribchester et al., 1995). Subsequent cross-breeding of *Wld*^{S} mice with mouse models of neuropathy and neurodegenerative disease, showed that *Wld*^{S} mitigates onset and progression of disease signs in some but not others, including mouse models of familial ALS (Ferri et al., 2003; Fischer et al., 2005; Kariya et al., 2008; Rose et al., 2008; Samsam et al., 2003; Vande Velde et al., 2004). This neuroprotective weakness may result from the age-dependent or gene dose-dependent decline in the capacity of Wld^S protein to adequately protect synapses (Gillingwater et al., 2002).

Thus, the fortuitous discovery of the *Wld*^{S} phenotype is highly instructive in several respects. First, it proves that beneficial, neuroprotective mutations may be undetectable using conventional screening methods based on clinical observation of behaviour. Second, it establishes a compelling and urgent case for systematic screening, in order to identify additional mutants with covert, neuroprotective phenotypes. Third, the benefits of one type of neuroprotective mutation may not be

Molecular and Cellular Neuroscience, Volume 42, Issue 4, November 2009, Pages 296–307
http://dx.doi.org/10.1016/j.mcn.2009.08.002

transferable to all forms of neurodegenerative disease, so one goal of systematic screening is to find mutations that are more effective in mitigating disease onset or progression than *Wld*^{S}. Finally, new methods are clearly required to carry out such systematic screening effectively if potentially-beneficial phenotypes are to be recognized unequivocally, in the absence of overt clinical signs.

Our principal aim in the present study was to find genetic modifiers that would enhance synaptic protection in *Wld*^{S} mice. In order to identify these modifiers (phenodeviants), we first developed a method for screening axonal and neuromuscular synaptic phenotypes in living mice based on fiber-optic confocal microendoscopy (CME; (Pelled et al., 2006; Vincent et al., 2006). We then induced genomic mutations using ethylnitrosourea (ENU) and screened for mutations that affected (enhanced or suppressed) axonal or synaptic degeneration in *Wld*^{S} mice using CME. Specifically, we crossbred ENU-mutagenized BALB/C mice with *thy1.2-YFP16/Wld*^{S} transgenic mice that express Yellow Fluorescent Protein (YFP) in motor neurons (Bridge et al., 2007; Feng et al., 2000) and employed CME to assess the preservation of morphology of axons and neuromuscular junctions following nerve section in the adult F1 offspring. Once the breeding pipeline for mutagenised mice had been established, the screen had a relatively high throughput (that is, it enabled *Wld*^{S}-modifiers to be identified on a shorter time scale than more conventional ENU-screening methods in mice). We identified several phenodeviants that were subsequently tested for inheritance, including re-assessment of axonal and neuromuscular synaptic protection using CME. We also extended the CME methodology to investigation of covert synaptic pathology in the well-established transgenic *SOD1*^{G93A} mouse model of ALS, which shows early onset of disease signs in motor axons and NMJ's (David et al., 2007; Frey et al., 2000; Gurney et al., 1994; Pun et al., 2006; Schaefer et al., 2005; Turner and Talbot, 2008). Finally we applied CME to the *ostes* mutant mouse, which was identified from a previous ENU-mutagenesis screen using standard SHIRPA screening protocols(Mackenzie et al., 2009), and which shows defects in axon regeneration (Mackenzie et al., 2007). Together, the results prove that CME and genomic mutagenesis can be combined in a powerful, flexible and versatile approach to investigation of neuromuscular biology and pathology at a cellular level *in vivo*.

Molecular and Cellular Neuroscience, Volume 42, Issue 4, November 2009, Pages 296–307
http://dx.doi.org/10.1016/j.mcn.2009.08.002

RESULTS

Neuromuscular synapses degenerate more rapidly in Wld^S heterozygotes than homozygotes.

We showed previously that in young adult (1-2 month old) homozygous *Wld^S* mice most neuromuscular synapses degenerate within 4-10 days of axotomy (Bridge et al., 2007; Gillingwater et al., 2002; Mack et al., 2001). Electrophysiological recording and analysis of neuromuscular synaptic transmission in double homozygous *thy1.2-YFP16:Wld^S* mice also showed no difference in the rate of synaptic degeneration following axotomy in these mice compared with those that did not express the YFP reporter (Bridge et al., 2007). Conventional confocal microscopy of muscles in *thy1.2-YFP16:Wld^S* mice supported these previous findings but additionally revealed striking differences in neuromuscular synaptic protection in *Wld^S* homozygotes compared with heterozygotes (Figure 1A-F). In this cohort, the rate of synaptic degeneration in *Wld^S* heterozgotes was virtually indistinguishable from that in wild-type mice: 24-48 hours after sciatic nerve section, motor endplates were vacant, uncovered by motor nerve terminals in both genotypes (Figure 1G). By 3 days there was therefore a clear distinction between almost complete preservation of motor nerve terminals in *Wld^S* homozyogtes, in contrast to almost complete synaptic degeneration in *Wld^S* heterozygotes. This distinction was evident despite indistinguishable levels of protection in the axotomized tibial nerve axons in homozygotes and heterozygotes at this time point (see below).

In light of the striking difference in synaptic protection in *Wld^S* heterozygotes and homozygotes, we envisaged using young adult heterozygous *Wld^S* mice as a sensitized background for seeking modifiers of axonal and synaptic degeneration. We reasoned also that a basal protective level of Wld^S protein, mitigating Wallerian degeneration of axons, would facilitate detection of protective mutations that might selectively suppress degeneration of synapses. In other words, normal Wallerian degeneration might obscure weak synaptic-protection phenotypes but Wld^S would delay this. Likewise, using *Wld^S* as a sensitised background also provided a more prolonged time-window for detecting mutations that might accelerate Wallerian degeneration of axons.

CME distinguishes intact from degenerating axons and synapses.

We developed a method for screening ENU-mutants, based on direct *in vivo* imaging of axons and neuromuscular junctions using fibre-optic confocal microendoscopy

Molecular and Cellular Neuroscience, Volume 42, Issue 4, November 2009, Pages 296–307
http://dx.doi.org/10.1016/j.mcn.2009.08.002

(CME). To validate this method, we first used CME to visualise intact axons and NMJ's in the tibial nerve on one side in *Wld*^{S} and wild-type mice, employing a standard, hand-held 1.5 mm diameter Proflex S-1500 optical-fiber probe. By manipulating the endoscopic probe tip through the same skin-aperture used to visualize the tibial nerve, we were able to visualize neuromuscular junctions (NMJ's) in the muscles adjacent to the tibial nerve, including the medial gastrocnemius muscle (Figure 2 A,B; Supplementary Movie 1). In order to minimise trauma, we took care not to force the probe tip through either the perineurial of epimysial sheaths. The probe tip was only applied to, manoeuvred and glided over the surfaces of the exposed tibial nerve and gastrocnemius muscle, through small (less than 5mm) incisions in the skin.

Next, we established that CME would allow us to recognise and distinguish protected from degenerating motor nerve terminals after unilateral section of the sciatic nerve under anaesthesia. We reanaesthetised mice 3 days after sciatic nerve section and used CME to image the distal axons in the tibial nerve and gastrocnemius NMJ's, as in unoperated mice. As expected (Gillingwater et al., 2002; Winlow and Usherwood, 1975), CME in *thy1.2-YFP16* mice – wild type for *Wld*^{S} - revealed that all the tibial nerve axons were fragmented and there were no intact axons or nerve terminals visible in 3-days denervated gastrocnemius muscle (n=11; Figure 2C). Also expected, the appearance of YFP-fluorescent axons in the 3-days axotomized distal tibial nerve of young adult homozygous *Wld*^{S} mice was similar to those of unoperated control mice and distinct from the fragmented appearance of degenerating axons in wild-type mice (compare Figures 2C and 2D). Intact motor nerve terminals were also readily observed in the axotomized gastrocnemius muscles of *thy1.2-YFP16/Wld*^{S} homozygous mice (Figure 2E; Supplementary Movie 2). However, axons and NMJ's in heterozygous *Wld*^{S} mice showed intact axons in the tibial nerve only (Figure 2D) with complete degeneration of intramuscular axons and motor nerve terminals in the gastrocnemius muscle (Figure 2F).

In further preparation for a mutagenesis screen, we established the likelihood of false-positives in heterozygous *Wld*^{S} mice: that is, spontaneous deviation from the characteristic phenotype (that is, synaptic protection being present 3 days after axotomy when it was expected to be absent in *Wld*^{S}/+ heterozygotes). In a sample of 20 F1-generation mice, produced by crossing BALB/c male mice with *thy1.2-YFP16/Wld*^{S} double-homozygous females, CME images showed intact axons and degenerated gastrocenmius NMJ's three days after axotomy in all of them. These

Molecular and Cellular Neuroscience, Volume 42, Issue 4, November 2009, Pages 296–307
http://dx.doi.org/10.1016/j.mcn.2009.08.002

data therefore suggest that the probability of observing synaptic protection by chance in a *Wld*^{S} heterozygote, 3 days after axotomy, is less than 5%. (Further data presented below suggest it is less than 2%). The data also indicated there is no constitutive enhancement or suppression of the *Wld*^{S}/+ phenotype in C57BL/6-BALB/c hybrid mice.

In sum, CME readily distinguishes intact axons and NMJ's from those undergoing Wallerian degeneration. We therefore concluded that *in vivo* imaging by CME at a single time point, 3 days after axotomy, would readily allow us to recognize the effects of additional genomic mutations, either in enhancing and accelerating axon degeneration, or in suppressing and retarding synaptic degeneration at NMJ's in *Wld*^{S} mice.

ENU induces modifiers of axonal and synaptic degeneration in Wld^S mice

Figure 3 shows the design of the modifier screen, which combined ENU mutagenesis in BALB/c mice, cross breeding with *thy1.2-YFP16/Wld*^{S} double-homozygotes; and then cutting the sciatic nerve in the 1-2 month old F1 offspring (heterozygous for *Wld*^{S}) and assessing the outcome 3 days later using CME. As described above, the tibial nerve and gastrocnemius muscle were exposed through a small skin incision and the tibial nerve axons and locations of NMJ's in gastrocnemius or other nearby muscles were examined using CME. We screened 219 F1 progeny of ENU-mutagenized mice on the sensitized *Wld*^{S}/+ background in accordance with this protocol. One of these mice evidently bore an ENU-induced mutation that constitutively produced an abnormally kinked tail. This incidence (approximately 1/200) of an overt phenotype endorses the efficacy of ENU as a mutagen in this cohort and is consistent with assessment using the SHIRPA methodology in previous ENU-screens (Nolan et al., 2000). None of the other mice showed any clinically overt phenotype with respect to their appearance or behaviour.

Seven mice in the ENU-mutagenized F1 cohort showed covert variations in synaptic or axonal phenotype compared with non-mutagenized *Wld*^{S}/+ mice. We classified these phenodeviants as CEMOP_S and CEMOP_A according to the respective cellular localization of the phenotype (CEMOP: **C**onfocal micro**E**ndoscopic **MO**toneuron **P**henotype; **_A**xons or **_S**ynapses). Mice CEMOP_S1 to S6 showed enhanced synaptic protection, varying from intact terminal axon branches and motor nerve terminals, to partial fragmentation of these presynaptic structures. Images of gastrocnemius NMJ's obtained from three of these mice are shown in Figure 4A-C

Molecular and Cellular Neuroscience, Volume 42, Issue 4, November 2009, Pages 296–307
http://dx.doi.org/10.1016/j.mcn.2009.08.002

and real-time imaging sequences from CEMOP_S2 and S5, which showed the strongest synaptic protection, are shown in Supplementary Movies 3 and 4. Subjectively, mice CEMOP_S3, S4 and S6 showed weaker synaptic protection than the others in this primary screen but nevertheless there was better protection in these phenodeviants than we have observed in any unmutagenized *Wld*^{S}/+ heterozygote (data not shown). Conversely, mouse CEMOP_A1 showed complete degeneration of neuromuscular synapses but also increased fragmentation of the axons (Figure 4D), indicating reduced protection of axons normally observed in *Wld*^{S}/+ heterozygotes: that is, enhancement of Wallerian degeneration. All the other F1 mice screened using CME displayed the characteristic neuromuscular phenotype expected of *Wld*^{S}/+ mice: that is, with intact tibial nerve axons but complete degeneration of motor innervation of gastrocnemius muscles. Almost all these phenotypcially-unremarkable mice were sacrificed before recovery from anaesthesia.

All seven phenodeviant, CEMOP_S1-6 and CEMOP_A1, mice were recovered from anaesthesia and crossed with either wild-type mice or *Wld*^{S} homozygotes to test for inheritance of their phenotypes. Mice from these F2 litters were anaesthetized at age 1-2 months and the sciatic nerve was sectioned unilaterally. They were reanaesthetized 3 days later and CME was used to visualize the tibial nerves and innervation of the gastrocnemius muscle, in the same fashion that was used to discover the founders.

The inheritance data are summarised in Table 1. Thus far, we have obtained compelling evidence for inheritance in two lines, CEMOP_S3 and CEMOP_S5 (Supplementary Figure S1; Supplementary Movie 5). None of the F2 mice that were negative for *Wld*^{S} in the litters showed evidence of synaptic protection. However, 4 out of 7 mice in the first litter from CEMOPS_5 that were genotyped as *Wld*^{S} heterozygotes (2 males and 2 females) showed evidence of synaptic protection 3 days after section of the sciatic nerve. Two additional litters derived from the CEMOPS_5 founder yielded a further 6 out 10 *Wld*^{S}/+ offspring that also showed neuromuscular synaptic protection at 3 days post axotomy. One of these mice was sacrificed and protection of neuromuscular synapses was confirmed in isolated lumbrical muscles using conventional confocal microscopy (Supplementary Figure S1). These ratios therefore constitute convincing evidence that line CEMOP_S5 carries an autosomal-dominant, ENU-induced mutation that delays synaptic degeneration, most likely by affecting the same pathways influenced by the neuroprotective mechanism of the *Wld*^{S} gene.

Molecular and Cellular Neuroscience, Volume 42, Issue 4, November 2009, Pages 296–307
http://dx.doi.org/10.1016/j.mcn.2009.08.002

Line CEMOP_S3 also showed evidence of inheritance but as yet we have insufficient data due to poor breeding and offspring-yield of the founder to conclude that this is Mendelian. Line CEMOP_S2 showed evidence of inheritance but, despite evidence of very strong synaptic protection in the founder (Figure 3B; Supplementary Movie 3), the numbers of offspring with a synaptic-protection phenotype (2/15 *Wld*^{S}/+ mice) suggesting only poor inheritance of the ENU-mutation, for which we are unable to provide a compelling explanation at present. In the remaining four CEMOP_S lines there was no evidence of inheritance of the deviant phenotype (Table 1). These four inheritance-negative mice are useful, however, because they allow us to place a revised, conservative upper bound of 4/219 (less than 2%) on the incidence of spontaneous phenodeviation with synaptic protection (ie phenotypic outliers) in *Wld*^{S}/+ heterozygous mice at 3 days post axotomy. By contrast, based on the number of offspring showing the same phenodeviation from the *Wld*^{S}/+ phenotype in the CEMOP_S5 line, the probability that the incidence of synaptic protection in the offspring derived from the founder was due to chance, rather than inheritance, is extremely low (less than 1.6×10^{-7}). This evidence therefore strongly suggests that CEMOP_S5 is a novel, Mendelian-dominant neuroprotective mutant that probably modifies the effect of *Wld*^{S} on its signalling pathways.

CME visualizes degenerating neuromuscular junctions in longitudinal studies of living mice

The discriminatory power of the CME technique led us naturally to inquire whether CME could be extended to longitudinal studies to monitor the degeneration of identified motor units, by repeated imaging of neuromuscular junctions in individual mice. We proved this principle both in *Wld*^{S} mice and in the *SOD1*^{G93A} transgenic mouse model of motor neuron disease.

Figure 5 shows a group of NMJ's identified in the flexor digitorum longus muscle, adjacent to the tibial nerve, in a homozygous *thy1.2-YFP16:Wld*^{S} mouse that was reanaesthetised and imaged at daily intervals, 3-5 days after sciatic nerve section. These images suggest that once synaptic degeneration is initiated in *Wld*^{S} motor units, the retraction of motor nerve terminals and degeneration of the axon collaterals that supply them can occur within less than 24 hrs.

Next, we applied CME to a preliminary study of neuromuscular synaptic degeneration in transgenic mice that incorporate a low number (7-15) of copies of the

Molecular and Cellular Neuroscience, Volume 42, Issue 4, November 2009, Pages 296–307
http://dx.doi.org/10.1016/j.mcn.2009.08.002

mutant human SOD1 gene, $SOD1^{G93A}$. These mice have a later onset and slower progression of disease than the more commonly-studied high (>20) copy-number strain (Alexander et al., 2004; Veldink et al., 2003). Low copy-number $SOD1^{G93A}$ mice begin to show abnormal motor reflexes and gait, or weakness in one or both hindlimbs, from about 4-10 months of age. We crossbred $SOD1^{G93A}$ transgenic mice with *thy1.2-YFP16* mice to generate the required fluorescent reporter in the diseased motor neurons.

CME was used to image NMJ's in two 3-month old (asymptomatic) and two 8-month old (symptomatic), double hemizygous *thy1.2-YFP16/*$SOD1^{G93A}$ mice. The older mice showed liminal abnormalities of gait and hindlimb weakness (one of these in shown in Supplementary Movie 6). The mice were anaesthetized and images of tibial nerve axons and gastrocnemius NMJ's were recorded. Four days later, the mice were re-anaesthetized and the tibial nerve axons and gastrocnemius NMJ's were re-examined. Intact axons and NMJ's were readily detected using CME in control, age-matched $SOD1^{G93A}$-negative mice that were littermates of the *thy1.2-YFP16/*$SOD1^{G93A}$ mice (Supplementary Figure S2). Validation was carried out by conventional confocal microscopy of isolated and fixed tibial nerves and hind limb muscles after sacrificing the animals at the end of the second viewing.

In the mouse shown in Supplementary Movie 6, a group of intramuscular collateral axon branches identified on initial viewing was re-identified during the second session. Some motor nerve terminals that were intact on the first viewing had evidently degenerated by the second (Figure 6 A,B; Supplementary Movies 7,8). Other NMJ's were supplied by thin or beaded preterminal axons. Sometimes collateral branches were completely disconnected from their original endplates (Figure 4C) referred to by others as a 'winter tree' appearance (Schaefer et al., 2005). Other junctions showed evidence of compensatory nerve terminal sprouting (Supplementary Figure S2). Thinning of preterminal axons and denervation of motor endplates was also observed in other muscles in these mice, verified *post mortem* using conventional confocal microscopy (Figure 4D). Although we also succeeded in relocating groups of NMJ's in the two 13-week old asymptomatic $SOD1^{G93A}$ we have not as yet found convincing evidence from CME that synapses undergo degeneration in advance of overt clinical signs of disease (data not shown).

These observations underscore the capability of CME to detect and monitor pathological signs of spontaneous synaptic degeneration in mice. It is most unlikely

Molecular and Cellular Neuroscience, Volume 42, Issue 4, November 2009, Pages 296–307
http://dx.doi.org/10.1016/j.mcn.2009.08.002

that degeneration of motor nerve terminals was caused by the CME imaging technique itself, for three main reasons. First, the neuromuscular abnormalities we observed were also present at neuromuscular junctions in end-stage SOD1^{G93A} mice that had not been subjected to CME (Figure 6E); second there was minimal possibility of mechanical damage by manipulation of the microendoscope itself because the short working distance of the probe required it to be glided over the surfaces of the exposed nerve and muscle, and we never penetrated the perineurial or epimysial sheaths with the probe tip. Third, in accordance with the above, most neuromuscular junctions examined in the SOD1^{G93A} mice, including those reimaged in asymptomatic mice, were unaltered by the repeated viewing and there was also no sign of axon degeneration following repeated imaging of the tibial nerve (Supplementary Figure S2).

CME captures slow axonal regeneration in ostes mice*.*

Finally, we asked whether CME was sensitive enough to monitor differences in peripheral nerve regeneration (Pelled et al., 2006; Vincent et al., 2006). For these experiments we imaged regenerating axons in the neuromuscular ENU-mutant *ostes,* identified in a separate dominant ENU screen using SHIRPA analysis (Nolan et al., 2000). These mice have an overt neurological phenotype (tremor and muscle weakness) and a complex underlying neuromuscular phenotype(Mackenzie et al., 2009). Independent experiments also demonstrated slow axon regeneration after peripheral nerve injury in homozygous *ostes* mice (Mackenzie et al., 2007). We compared axonal regeneration in *thy1.2-YFP16*:*ostes* in homozygotes, heterozygotes and their age-matched wild-type littermates. The mice were re-anaesthetized 10-30 days after unilateral sciatic nerve crush and the axons and neuromuscular junctions of the distal tibial nerve and gastrocnemius muscles were exposed through small skin apertures as described above.

CME confirmed the delayed axonal regeneration in homozygous and heterozygous *ostes* mice (Figure 7A-C). By 10 days, few regenerating axons had reached the tibial nerve in *ostes/*+ heterozygotes compared with wild-type littermates and none had regenerated in homozygotes. This was verified *post mortem,* by conventional confocal microscopy of the tibial nerve (Figure 7D-F). By 20 days, CME of the tibial nerve indicated similar levels of regeneration in all three groups of mice (Supplementary Figure S3) but conventional microscopy of lumbrical muscles showed most endplates reinnervated only in wild-type and *ostes/*+ heterozygotes (Figure 7G-I). By 30 days, virtually all motor endplates in the lumbrical muscles of

Molecular and Cellular Neuroscience, Volume 42, Issue 4, November 2009, Pages 296–307
http://dx.doi.org/10.1016/j.mcn.2009.08.002

the *ostes/+* heterozygotes were reinnervated but *ostes/ostes* homozygotes still showed fewer reinnervated endplates (data not shown).

DISCUSSION

We have shown here how ENU-mutagenesis when combined with CME establishes an effective platform for identifying covert deviations in the pattern or rate of axonal and neuromuscular synaptic degeneration and regeneration. The phenodeviants and mutants we identified in the *Wld*^{S}-modifier screen would have been undetectable using conventional screening methods. The potential diagnostic value of CME is also underscored by the proof that that this technique enables minimally-invasive, longitudinal imaging of axons or motor nerve terminals undergoing degeneration and regeneration following nerve injury, or in an animal model of ALS. Several studies suggest that widespread malfunction or degeneration of motor axons and their terminals occur in neurodegenerative diseases before overt impairment of motor function is detected (David et al., 2007; Fischer et al., 2004; Frey et al., 2000; Gurney et al., 1994; Pun et al., 2006; Ravits et al., 2007; Schaefer et al., 2005). Further developments of CME technology and identification of the mechanisms of synaptic protection in the mutants we identify using it may therefore provided a basis for robust or routine examination then monitoring of treatment from early stages in progression of neuromuscular disease.

Our screening method has potential for high throughput: with the present design and, once a pipeline of breeding and surgical preparation is established, a trained single investigator can readily screen between 10-20 mutagenised mouse lines per day, a rate we achieved towards the end of the present study (see Methods). The number of phenodeviants we detected (7 out of 219 ENU/*Wld*^{S} mice screened) is consistent with the incidence of phenodeviation in other modifier screens (Carpinelli et al., 2004; Rubio-Aliaga et al., 2007). Not all these phenodeviants showed germ-line transmission of their phenotypes, however. Failure of inheritance tests following detection of phenodeviants in founder animals sometimes is a general feature of modifier-screens perhaps owing to polygenic inheritance, a background-sensitive low penetrance mutation, or the result of a stochastic event (P.Nolan, personal communication). However, our compelling evidence for inheritance of mutations that protects synapses, especially in the CEMOP_S5 line, both vindicates and validates CME as a basis for rapid screening for covert phenotypes.

Molecular and Cellular Neuroscience, Volume 42, Issue 4, November 2009, Pages 296–307
http://dx.doi.org/10.1016/j.mcn.2009.08.002

How useful might the modifiers of synaptic degeneration we identified become? Transfer of *Wld*^{S} expression itself has proved to be ineffective on disease onset or progression by ectopic expression in transgenic mouse models of ALS (Fischer et al., 2005; Vande Velde et al., 2004) or spinal muscular atrophy (Kariya et al., 2008; Rose et al., 2008), although caution should be exercised in interpreting any lack of protective effects on NMJ's when only a single allele of *Wld*^{S} is present (ie in heterozygotes); or where disease signs are of late onset, owing to the weak protection of axons and NMJ's conferred by *Wld*^{S} in aged mice (Fischer et al., 2005; Gillingwater et al., 2002; Perry et al., 1992; Ribchester et al., 1995). However, co-expression of *Wld*^{S} has been shown to partially block degeneration in axonal disorders including dysmyelination (Samsam et al., 2003), motor neuropathy (Ferri et al., 2003), axonal spheroid pathology (Mi et al., 2005) and taxol toxicity (Wang et al., 2002). It remains to be shown whether the protective benefits of CEMOP_S5 can be transferred to mouse models of ALS or other neurodegenerative diseases. Continued screening for similar covert mutant phenotypes is also warranted, to maximize chances of detecting additional mutations, only some of whose effects might be sufficient to arrest disease progression in animal models of disease (see, for example, Kieran et al., 2005). Thus, we may anticipate that one or more mutations identified by combining mutagenesis with CME will lead to significant improvements in protection of neuromuscular synapses, increasing the resources that might ultimately be used to understand or treat neuromuscular disease.

Why seek modifiers in a model of delayed Wallerian degeneration (*Wld*^{S} mice) rather than, for example, in the well-established SOD1^{G93A} animal model of ALS? The main reason is that the *Wld*^{S} mutation is well suited as a sensitized background for detection of modifiers of axonal or synaptic degeneration, because the onset of degeneration is triggered simultaneously in all axons by a surgical nerve lesion. Degeneration then progresses over a well-defined, relatively brief time course with little heterogeneity between axons (Beirowski et al., 2005; Beirowski et al., 2004; Bridge et al., 2007; Gillingwater et al., 2002). A modified form of our experimental design could have been used, in principle, to find beneficial modifiers of early neuromuscular synaptic and axonal degeneration in SOD1^{G93A} mutant mice (David et al., 2007; Fischer et al., 2004; Pun et al., 2006; Schaefer et al., 2005) and perhaps now this should be attempted. However, the unpredictable variation in the onset and endpoints of disease in SOD1^{G93A} mice places significant additional constraints on the design of screens that might be capable of detecting deviations from stages in the disease progression (Benatar, 2007; Schnabel, 2008; Scott et al., 2008).

Molecular and Cellular Neuroscience, Volume 42, Issue 4, November 2009, Pages 296–307
http://dx.doi.org/10.1016/j.mcn.2009.08.002

Refinement of the CME method and its application to longitudinal study and monitoring of disease signs in mouse models of ALS offers an attractive prospect for overcoming the limitations in interpretation of most studies on $SOD1^{G93A}$ transgenic mice due to variability in the onset of disease signs in this line.

The physiological mechanisms of action of mutations such CEMOP_S5 - or others arising from the mutatgenesis screen – could, like Wld^S, involve modification of transcription or translation of other genes (Gillingwater et al., 2006; Wishart et al., 2007b); or by direct modification of intracellular signalling (see (Beirowski et al., 2009; Conforti et al., 2007; Wilbrey et al., 2008); or by targeting enzymic activity to intracellular compartments that are pivotal in regulating energy metabolism (Conforti et al., 2009). Establishing the gene mutations will be the most important step towards identifying their mechanism of action. The discovery and analysis of the spontaneous Wld^S mutant, though more complex than a point mutation, is instructive. The phenotype was discovered serendipitously. The gene was then identified, by positional cloning then reconstitution of phenotype in transgenic mice (Coleman et al., 1998; Lunn et al., 1989; Lyon et al., 1993; Mack et al., 2001). A similar strategy has been successfully used to establish the locus of point mutations that produce neurodegeneration (Kieran et al., 2005); Mackenzie et al., 2009). Recent methodologies for high-throughput, fast genomic sequencing may facilitate the identification the locus and nature of the mutation in the CEMOPS_5 and CEMOPS_3 mutants identified by the present screening method (Olson, 2007).

We have also shown that CME is a viable technique for monitoring differences in axon regeneration in mutants *in vivo.* It is possible to monitor axon degeneration and regeneration non-invasively in small mammals at low resolution using techniques ranging from transcutaneous imaging with a fluorescence dissecting microscope (Pan et al., 2003) to magnetic resonance imaging (Bendszus and Stoll, 2005). Although CME is more invasive, it provides the optical resolution required to visualize single axons, and to distinguish fragmented, degenerating axons from thin, regenerating axons (Schaefer et al., 2005), as well as capacity to detect abnormalities in the form of regenerating neuromuscular synapses. Neither of these can be resolved with present non-invasive, low-resolution methods. The *ostes*/+ mice we studied here demonstrate the facility for CME to detect mutants that show deviations from normal patterns or the rate of axon regeneration and these mice themselves represent a potentially powerful resource as a sensitized genetic

Molecular and Cellular Neuroscience, Volume 42, Issue 4, November 2009, Pages 296–307
http://dx.doi.org/10.1016/j.mcn.2009.08.002

background for a further ENU mutagenesis screen, designed to expose novel covert motor neuron regeneration phenotypes.

How suitable might CME be for visualizing subtle defects in neuromuscular pathology *in vivo*? Visualization of neuromuscular junctions *in vivo* using conventional fluorescence microscopy has been established over many years as a technique for repeated imaging and has yielded considerable biological insights into the plasticity of NMJ's in development, aging and disease (Balice-Gordon and Lichtman, 1990; Misgeld and Kerschensteiner, 2006; Schaefer et al., 2005; Walsh and Lichtman, 2003). Recently, mulitphoton-microscopy using gradient refractive-index (GRIN) lenses, has successfully been applied to visualisation of muscle structure and function in mice and humans (Barretto et al., 2009; Llewellyn et al., 2008). While the CME method has a theoretical spatial resolution of only 2-5 μm, which is much lower than either conventional water immersion objectives or GRIN lenses, it has the advantages of being faster, less invasive and more versatile than either conventional confocal or multiphoton microscopy. For instance, imaging NMJ using conventional optics requires stabilization and artificial ventilation of a deeply anaesthetized animal, with exposure of a relatively large area of muscle to admit the tip of a long-working distance water-dipping objective. Mice enduring this invasive and relatively lengthy procedure are likely to be at higher risk of subsequent health problems; and animal welfare is of paramount concern for the viability of the line, not least the capacity to test for inheritance of a deviant phenotype and to generate sufficient mice for mapping and identifying the mutation. Multiphoton imaging via GRIN lenses has been shown to be feasible in mice and in humans but with limited flexibility and requiring sensitive, specialized (and relatively expensive) equipment. By contrast, CME is flexible, minimally-invasive and therefore suitable for high-throughput, genome-wide mutagenesis screening and for longitudinal investigation of neuromuscular abnormalities. The probe diameter is smaller than most biopsy needles (Tobina et al., 2009). Thus, a variant of the CME method may prove suitable for longitudinal examination of NMJ's in humans.

In summary, we have shown that mutants with covert enhancement or suppression of synaptic degeneration can be produced by ENU-mutagenesis, supporting the hypothesis that degeneration of synaptic terminals is regulated differently and perhaps independently from that of axons or neuronal cell bodies (Gillingwater & Ribchester, 2001, 2003). CME is a practical method for visualising synaptic degeneration *in vivo;* and longitudinal study of covert neuromuscular phenotypes can

Molecular and Cellular Neuroscience, Volume 42, Issue 4, November 2009, Pages 296–307
http://dx.doi.org/10.1016/j.mcn.2009.08.002

be efficiently performed using this flexible and minimally-invasive imaging technique. In the long run, the biological resources generated in the present study and future applications of CME may lead to more effective monitoring and treatment of neuromuscular disease.

EXPERIMENTAL METHODS

Mouse strains

The strains used included: BALB/c mice (Charles River); *Wld*^{S} mutant mice on a C57BL/6 background (Harlan UK); transgenic mouse line *thy1.2-YFP16* (Feng et al., 2000); a low (7-15) copy-number strain of SOD1^{G93A} transgenic mice, specifically B6.Cg-Tg(SOD1-G93A)1Gur/J (Jackson Laboratory, Bar Harbor, Maine), carrying the G93A mutant form of the human SOD1 transgene; and *ostes* mice identified in a separate ENU-mutagenesis screen and established on a mixed BALB/c:FVB background (Mackenzie et al., 2009) . Mutagenized mice were produced following a protocol of ENU injection in BALB/C male mice as previously described (Justice et al., 2000). *Wld*^{S} mice were bred to homozygosity into *thy1.2-YFP16* mice by recurrent backcrosses to generate double homozygotes for *Wld*^{S} and *thy1.2-YFP16*. *YFP16:SOD1*^{G93A} lines were established by breeding fertile SOD1^{G93A} males with homozygous *thy1.2-YFP16* females. Similarly, *ostes* mice were also crossed with the transgenic line *thy1.2-YFP16* to generate homozygous and heterozygous *ostes* mice with fluorescent motor neurons. Animal studies were conducted under the guidance issued by the UK Medical Research Council (*Medical Research Council Responsibility In the Use of Animals for Medical Research* (Medical Research Council, London, 1993)) and UK Home Office Welfare guidelines (Home Office Project Licence no. 30/2287). Mice had free access to water (25 ppm chlorine) and were fed *ad libitum* on a commercial diet (SDS maintenance diet) containing 2.6% saturated fat.

DNA Extraction and Genotyping

Mice were genotyped for *Wld*^{S} using quantitative real-time PCR (Wishart et al., 2007a). For genotyping SOD1^{G93A} mice, genomic DNA was extracted from earclips using alkaline lysis in 50mM NaOH. Mice were genotyped for human SOD1G93A, using primers 5'-CAT CAG CCC TAA TCC ATC TGA-3' and 5'-CGC GAC TAA CAA TCA AAG TGA-3' (236bp product)(Rosen et al., 1993) and mouse alpha- Synuclein

Molecular and Cellular Neuroscience, Volume 42, Issue 4, November 2009, Pages 296–307
http://dx.doi.org/10.1016/j.mcn.2009.08.002

5'-AGA AGA CCA AAG AGC AAG TGA CA-3' and 5'-ATC TGG TCC TTC TTG ACA AAG C-3' (130bp product) as an internal control. PCR amplification was performed using Platinum PFX (Invitrogen, Paisley, UK) in 2x amplification buffer and the PCR products, 130bp and 236bp respectively, were separated by agarose gel electrophoresis. For *Wld*^{S} and *ostes* mouse genotyping, genomic DNA was extracted from mouse tail tips using Nucleon BACC2 DNA purification kit (Tepnel Life Sciences PLC) according to manufacturer's instructions with the following modifications: 1) tail tips of 2.5mm were directly placed in 200μl of Reagent B, Proteinase K was added at 200 μg/ml and the mixture incubated overnight at 55°C. 2) DNA was resuspended in 50 μl of double-distilled water and stored at -20°C as a stock solution. *Ostes* mice were genotyped by PCR amplification and analysed by single-stranded conformational polymorphism (SSCP) using the following primers: TGGTA GAAGA GAACC CACTT CC (forward) and TCTTT ACTCA TGGTT GGTGC AT (reverse). Mice carrying the *thy1.2-YFP16* transgene were identified by the presence of fluorescent axons in fresh ear-punches, using a standard fluorescence compound microscope.

Surgery

Mice were prepared for surgery with a subcutaneous injection of 100 μl of Vetergesic® (buprenorphine 4.2μg/ml) following anaesthesia by inhalation of 3-5% isoflurane/O_2 (1 litre/min). The sciatic nerve was exposed unilaterally through a small incision at mid-thigh level and the nerve either sectioned with scissors or crushed firmly between the jaws of watchmakers forceps for 30s. The continuity of the perineurial sheath of the sciatic nerve after nerve crush was checked *in situ*. Skin wounds were closed with silk suture.

Analysis of axonal and synaptic morphology

For *in vivo* analysis, severed sciatic nerve axons located distally in the tibial nerve and superficial neuromuscular junctions in the gastrocnemius muscle were visualized via a small (<5 mm) incision in the skin. A Proflex S-1500 fiber-optic probe with a tip diameter of 1500 μm was connected to either Mauna Kea Technologies CellVizio or Leica FCM1000 confocal microendoscopes. The laser scanning units had an excitation wavelength of 488 nm with a collection bandwidth of 505 nm – 700 nm. Images were captured at 12 frames/second The probe tip was normally manipulated by hand through the skin wound while monitoring the images acquired in real time using ImageCell software running on Apple Mac computers supplied with the

Molecular and Cellular Neuroscience, Volume 42, Issue 4, November 2009, Pages 296–307
http://dx.doi.org/10.1016/j.mcn.2009.08.002

instrument. Once we had established the routine procedure for the screen, the mean time of the final imaging session, from induction of anaesthesia through CME imaging, appraisal of axonal and neuromuscular phenotype, to wound-suture and recovery or sacrifice of the mouse, was 12.5±1.8 minutes (mean±S.D.) per mouse. Conventional confocal microscopy was performed on whole mounts fixed in 4 % paraformaldehyde for 30-60 minutes, counterstained with TRITC-α-bungarotoxin to label acetylcholine receptors, washed in phosphate-buffered saline and mounted in Vectashield or Mowiol, using either a Leica SP5 or BioRad Radiance 2000 confocal microscopes. Scoring of endplate occupancy was normally done at low power (4x-20x objectives) while viewing with conventional fluorescence optics, or from montages of whole muscles made by digital stitching of contiguous z-series obtained using the confocal microscope. An endplate was scored as vacant if there was no discernible evidence of any contact by an overlying YFP-positive motor nerve terminal with the TRITC-α-bungarotoxin stained motor endplate area.

Acknowledgements

This work was supported by grants from the Medical Research Council, the Motor Neurone Disease Association and MND Scotland. We thank Drs A. Acevedo, S. Brown, L. Conforti, T.H. Gillingwater, P.Nolan and S.H. Parson for discussions and helpful comments on the manscript; Drs A. Acevedo and T. Wishart for advice and assistance with genotyping; and L. Ireson and S. Polley for assistance with animal care and mutagenesis.

Molecular and Cellular Neuroscience, Volume 42, Issue 4, November 2009, Pages 296–307
http://dx.doi.org/10.1016/j.mcn.2009.08.002

References

Acevedo-Arozena, A., Wells, S., Potter, P., Kelly, M., Cox, R.D., Brown, S.D., 2008. ENU mutagenesis, a way forward to understand gene function. Annual review of genomics and human genetics 9, 49-69.

Alexander, G.M., Erwin, K.L., Byers, N., Deitch, J.S., Augelli, B.J., Blankenhorn, E.P., Heiman-Patterson, T.D., 2004. Effect of transgene copy number on survival in the G93A SOD1 transgenic mouse model of ALS. Brain research 130, 7-15.

Balice-Gordon, R.J., Lichtman, J.W., 1990. In vivo visualization of the growth of pre- and postsynaptic elements of neuromuscular junctions in the mouse. J Neurosci 10, 894-908.

Barretto, R.P., Messerschmidt, B., Schnitzer, M.J., 2009. In vivo fluorescence imaging with high-resolution microlenses. Nature methods 6, 511-512.

Beirowski, B., Adalbert, R., Wagner, D., Grumme, D.S., Addicks, K., Ribchester, R.R., Coleman, M.P., 2005. The progressive nature of Wallerian degeneration in wild-type and slow Wallerian degeneration (WldS) nerves. BMC neuroscience 6, 6.

Beirowski, B., Babetto, E., Gilley, J., F., M., Conforti, L., Janeckova, L., Magni, G., Ribchester, R., Coleman, M., 2009. Non-nuclear WldS determines its neuroprotective efficacy for axons and synapses. J Neurosci In Press.

Beirowski, B., Berek, L., Adalbert, R., Wagner, D., Grumme, D.S., Addicks, K., Ribchester, R.R., Coleman, M.P., 2004. Quantitative and qualitative analysis of Wallerian degeneration using restricted axonal labelling in YFP-H mice. Journal of neuroscience methods 134, 23-35.

Benatar, M., 2007. Lost in translation: treatment trials in the SOD1 mouse and in human ALS. Neurobiology of disease 26, 1-13.

Bendszus, M., Stoll, G., 2005. Technology insight: visualizing peripheral nerve injury using MRI. Nature clinical practice 1, 45-53.

Bridge, K.E., Berg, N., Adalbert, R., Babetto, E., Dias, T., Spillantini, M.G., Ribchester, R.R., Coleman, M.P., 2007. Late onset distal axonal swelling in YFP-H transgenic mice. Neurobiology of aging.

Bruijn, L.I., Cleveland, D.W., 1996. Mechanisms of selective motor neuron death in ALS: insights from transgenic mouse models of motor neuron disease. Neuropathology and applied neurobiology 22, 373-387.

Bruijn, L.I., Miller, T.M., Cleveland, D.W., 2004. Unraveling the mechanisms involved in motor neuron degeneration in ALS. Annual review of neuroscience 27, 723-749.

Carpinelli, M.R., Hilton, D.J., Metcalf, D., Antonchuk, J.L., Hyland, C.D., Mifsud, S.L., Di Rago, L., Hilton, A.A., Willson, T.A., Roberts, A.W., Ramsay, R.G., Nicola, N.A., Alexander, W.S., 2004. Suppressor screen in Mpl-/- mice: c-Myb mutation causes supraphysiological production of platelets in the absence of thrombopoietin signaling. Proceedings of the National Academy of Sciences of the United States of America 101, 6553-6558.

Coleman, M.P., Conforti, L., Buckmaster, E.A., Tarlton, A., Ewing, R.M., Brown, M.C., Lyon, M.F., Perry, V.H., 1998. An 85-kb tandem triplication in the slow Wallerian degeneration (Wlds) mouse. Proceedings of the National Academy of Sciences of the United States of America 95, 9985-9990.

Conforti, L., Fang, G., Beirowski, B., Wang, M.S., Sorci, L., Asress, S., Adalbert, R., Silva, A., Bridge, K., Huang, X.P., Magni, G., Glass, J.D., Coleman, M.P., 2007. NAD(+) and axon degeneration revisited: Nmnat1 cannot substitute for Wld(S) to delay Wallerian degeneration. Cell death and differentiation 14, 116-127.

Conforti, L., Tarlton, A., Mack, T.G., Mi, W., Buckmaster, E.A., Wagner, D., Perry, V.H., Coleman, M.P., 2000. A Ufd2/D4Cole1e chimeric protein and overexpression of Rbp7 in the slow Wallerian degeneration (WldS) mouse. Proceedings of the National Academy of Sciences of the United States of America 97, 11377-11382.

Conforti, L., Wilbrey, A., Morreale, G., Janeckova, L., Beirowski, B., Adalbert, R., Mazzola, F., Di Stefano, M., Hartley, R., Babetto, E., Smith, T., Gilley, J., Billington, R.A., Genazzani, A.A., Ribchester, R.R., Magni, G., Coleman, M., 2009. Wld S protein requires Nmnat activity and a short N-terminal sequence to protect axons in mice. The Journal of cell biology 184, 491-500.

Cook, M.C., Vinuesa, C.G., Goodnow, C.C., 2006. ENU-mutagenesis: insight into immune function and pathology. Current opinion in immunology 18, 627-633.
David, G., Nguyen, K., Barrett, E.F., 2007. Early vulnerability to ischemia/reperfusion injury in motor terminals innervating fast muscles of SOD1-G93A mice. Experimental neurology 204, 411-420.

Feng, G., Mellor, R.H., Bernstein, M., Keller-Peck, C., Nguyen, Q.T., Wallace, M., Nerbonne, J.M., Lichtman, J.W., Sanes, J.R., 2000. Imaging neuronal subsets in transgenic mice expressing multiple spectral variants of GFP. Neuron 28, 41-51.

Ferri, A., Sanes, J.R., Coleman, M.P., Cunningham, J.M., Kato, A.C., 2003. Inhibiting axon degeneration and synapse loss attenuates apoptosis and disease progression in a mouse model of motoneuron disease. Curr Biol 13, 669-673.

Fischer, L.R., Culver, D.G., Davis, A.A., Tennant, P., Wang, M., Coleman, M., Asress, S., Adalbert, R., Alexander, G.M., Glass, J.D., 2005. The WldS gene modestly prolongs survival in the SOD1G93A fALS mouse. Neurobiology of disease 19, 293-300.

Fischer, L.R., Culver, D.G., Tennant, P., Davis, A.A., Wang, M., Castellano-Sanchez, A., Khan, J., Polak, M.A., Glass, J.D., 2004. Amyotrophic lateral sclerosis is a distal axonopathy: evidence in mice and man. Experimental neurology 185, 232-240.

Frey, D., Schneider, C., Xu, L., Borg, J., Spooren, W., Caroni, P., 2000. Early and selective loss of neuromuscular synapse subtypes with low sprouting competence in motoneuron diseases. J Neurosci 20, 2534-2542.

Gillingwater, T.H., Ribchester, R.R., 2001. Compartmental neurodegeneration and synaptic plasticity in the Wld(s) mutant mouse. The Journal of physiology 534, 627-639.

Gillingwater, T.H., Thomson, D., Mack, T.G., Soffin, E.M., Mattison, R.J., Coleman, M.P., Ribchester, R.R., 2002. Age-dependent synapse withdrawal at axotomised neuromuscular junctions in Wld(s) mutant and Ube4b/Nmnat transgenic mice. The Journal of physiology 543, 739-755.

Gillingwater, T.H., Wishart, T.M., Chen, P.E., Haley, J.E., Robertson, K., MacDonald, S.H., Middleton, S., Wawrowski, K., Shipston, M.J., Melmed, S., Wyllie, D.J., Skehel, P.A., Coleman, M.P., Ribchester, R.R., 2006. The neuroprotective WldS gene regulates expression of PTTG1 and erythroid differentiation regulator 1-like gene in mice and human cells. Human molecular genetics 15, 625-635.

Godinho, S.I., Nolan, P.M., 2006. The role of mutagenesis in defining genes in behaviour. Eur J Hum Genet 14, 651-659.

Gondo, Y., 2008. Trends in large-scale mouse mutagenesis: from genetics to functional genomics. Nat Rev Genet 9, 803-810.

Gotz, J., Deters, N., Doldissen, A., Bokhari, L., Ke, Y., Wiesner, A., Schonrock, N., Ittner, L.M., 2007. A decade of tau transgenic animal models and beyond. Brain pathology (Zurich, Switzerland) 17, 91-103.

Gotz, J., Ittner, L.M., 2008. Animal models of Alzheimer's disease and frontotemporal dementia. Nature reviews 9, 532-544.

Gurney, M.E., Pu, H., Chiu, A.Y., Dal Canto, M.C., Polchow, C.Y., Alexander, D.D., Caliendo, J., Hentati, A., Kwon, Y.W., Deng, H.X., et al., 1994. Motor neuron degeneration in mice that express a human Cu,Zn superoxide dismutase mutation. Science (New York, N.Y 264, 1772-1775.

Jackson, M., Ganel, R., Rothstein, J.D., 2002. Models of amyotrophic lateral sclerosis. Current protocols in neuroscience / editorial board, Jacqueline N. Crawley ... [et al Chapter 9, Unit 9 13.

Justice, M.J., Carpenter, D.A., Favor, J., Neuhauser-Klaus, A., Hrabe de Angelis, M., Soewarto, D., Moser, A., Cordes, S., Miller, D., Chapman, V., Weber, J.S., Rinchik, E.M., Hunsicker, P.R., Russell, W.L., Bode, V.C., 2000. Effects of ENU dosage on mouse strains. Mamm Genome 11, 484-488.

Kariya, S., Mauricio, R., Dai, Y., Monani, U.R., 2008. The neuroprotective factor Wld(s) fails to mitigate distal axonal and neuromuscular junction (NMJ) defects in mouse models of spinal muscular atrophy. Neuroscience letters.

Kieran, D., Hafezparast, M., Bohnert, S., Dick, J.R., Martin, J., Schiavo, G., Fisher, E.M., Greensmith, L., 2005. A mutation in dynein rescues axonal transport defects and extends the life span of ALS mice. The Journal of cell biology 169, 561-567.

Llewellyn, M.E., Barretto, R.P., Delp, S.L., Schnitzer, M.J., 2008. Minimally invasive high-speed imaging of sarcomere contractile dynamics in mice and humans. Nature 454, 784-788.

Lunn, E.R., Brown, M.C., Perry, V.H., 1990. The pattern of axonal degeneration in the peripheral nervous system varies with different types of lesion. Neuroscience 35, 157-165.

Lunn, E.R., Perry, V.H., Brown, M.C., Rosen, H., Gordon, S., 1989. Absence of Wallerian Degeneration does not Hinder Regeneration in Peripheral Nerve. The European journal of neuroscience 1, 27-33.

Lyon, M.F., Ogunkolade, B.W., Brown, M.C., Atherton, D.J., Perry, V.H., 1993. A gene affecting Wallerian nerve degeneration maps distally on mouse chromosome 4. Proceedings of the National Academy of Sciences of the United States of America 90, 9717-9720.

Mack, T.G., Reiner, M., Beirowski, B., Mi, W., Emanuelli, M., Wagner, D., Thomson, D., Gillingwater, T., Court, F., Conforti, L., Fernando, F.S., Tarlton, A., Andressen, C., Addicks, K., Magni, G., Ribchester, R.R., Perry, V.H., Coleman, M.P., 2001. Wallerian degeneration of injured axons and synapses is delayed by a Ube4b/Nmnat chimeric gene. Nature neuroscience 4, 1199-1206.

Mackenzie, F., Ribchester, R., Gillingwater, T., Powles-Glover, N., Gale, R., Wong, F., Arkell, R., Blanco, G., 2007. Identification and characterisation of a candidate gene for ostes, a novel mouse mutant showing muscle denervation and atrophy. Amyotroph Lateral Scler 8, Supplement 1, 1.

Mackenzie, F.E., Romero, R., Wong, F., Williams, D., Gillingwater, T., Hilton, H., Dick, J., Riddoch-Contereras, J., Ireson, L., Powles-Glover, N., Riley, G., Underhill, P., Hough, T., Arkell, R., Greensmith, L., Ribchester, R.R., Blanco, G., 2009. Upregulation of PKD1L2 provokes a complex neuromuscular disease in the mouse. Human molecular genetics.

Mi, W., Beirowski, B., Gillingwater, T.H., Adalbert, R., Wagner, D., Grumme, D., Osaka, H., Conforti, L., Arnhold, S., Addicks, K., Wada, K., Ribchester, R.R., Coleman, M.P., 2005. The slow Wallerian degeneration gene, WldS, inhibits axonal spheroid pathology in gracile axonal dystrophy mice. Brain 128, 405-416.

Misgeld, T., Kerschensteiner, M., 2006. In vivo imaging of the diseased nervous system. Nature reviews 7, 449-463.

Nolan, P.M., Peters, J., Vizor, L., Strivens, M., Washbourne, R., Hough, T., Wells, C., Glenister, P., Thornton, C., Martin, J., Fisher, E., Rogers, D., Hagan, J., Reavill, C., Gray, I., Wood, J., Spurr, N., Browne, M., Rastan, S., Hunter, J., Brown, S.D., 2000. Implementation of a large-scale ENU mutagenesis program: towards increasing the mouse mutant resource. Mamm Genome 11, 500-506.

Olson, M., 2007. Enrichment of super-sized resequencing targets from the human genome. Nature methods 4, 891-892.

Pan, Y.A., Misgeld, T., Lichtman, J.W., Sanes, J.R., 2003. Effects of neurotoxic and neuroprotective agents on peripheral nerve regeneration assayed by time-lapse imaging in vivo. J Neurosci 23, 11479-11488.

Pelled, G., Dodd, S.J., Koretsky, A.P., 2006. Catheter confocal fluorescence imaging and functional magnetic resonance imaging of local and systems level recovery in the regenerating rodent sciatic nerve. NeuroImage 30, 847-856.

Perry, V.H., Brown, M.C., Lunn, E.R., Tree, P., Gordon, S., 1990a. Evidence that Very Slow Wallerian Degeneration in C57BL/Ola Mice is an Intrinsic Property of the Peripheral Nerve. The European journal of neuroscience 2, 802-808.

Perry, V.H., Brown, M.C., Tsao, J.W., 1992. The Effectiveness of the Gene Which Slows the Rate of Wallerian Degeneration in C57BL/Ola Mice Declines With Age. The European journal of neuroscience 4, 1000-1002.

Perry, V.H., Lunn, E.R., Brown, M.C., Cahusac, S., Gordon, S., 1990b. Evidence that the Rate of Wallerian Degeneration is Controlled by a Single Autosomal Dominant Gene. The European journal of neuroscience 2, 408-413.

Pun, S., Santos, A.F., Saxena, S., Xu, L., Caroni, P., 2006. Selective vulnerability and pruning of phasic motoneuron axons in motoneuron disease alleviated by CNTF. Nature neuroscience 9, 408-419.

Ravits, J., Laurie, P., Fan, Y., Moore, D.H., 2007. Implications of ALS focality: rostral-caudal distribution of lower motor neuron loss postmortem. Neurology 68, 1576-1582.

Ribchester, R.R., Tsao, J.W., Barry, J.A., Asgari-Jirhandeh, N., Perry, V.H., Brown, M.C., 1995. Persistence of neuromuscular junctions after axotomy in mice with slow Wallerian degeneration (C57BL/WldS). The European journal of neuroscience 7, 1641-1650.

Rose, F.F., Jr., Meehan, P.W., Coady, T.H., Garcia, V.B., Garcia, M.L., Lorson, C.L., 2008. The Wallerian degeneration slow (Wld(s)) gene does not attenuate disease in a mouse model of spinal muscular atrophy. Biochemical and biophysical research communications 375, 119-123.

Rosen, D.R., Siddique, T., Patterson, D., Figlewicz, D.A., Sapp, P., Hentati, A., Donaldson, D., Goto, J., O'Regan, J.P., Deng, H.X., et al., 1993. Mutations in Cu/Zn

superoxide dismutase gene are associated with familial amyotrophic lateral sclerosis. Nature 362, 59-62.

Rubio-Aliaga, I., Soewarto, D., Wagner, S., Klaften, M., Fuchs, H., Kalaydjiev, S., Busch, D.H., Klempt, M., Rathkolb, B., Wolf, E., Abe, K., Zeiser, S., Przemeck, G.K., Beckers, J., de Angelis, M.H., 2007. A genetic screen for modifiers of the delta1-dependent notch signaling function in the mouse. Genetics 175, 1451-1463.

Samsam, M., Mi, W., Wessig, C., Zielasek, J., Toyka, K.V., Coleman, M.P., Martini, R., 2003. The Wlds mutation delays robust loss of motor and sensory axons in a genetic model for myelin-related axonopathy. J Neurosci 23, 2833-2839.

Schaefer, A.M., Sanes, J.R., Lichtman, J.W., 2005. A compensatory subpopulation of motor neurons in a mouse model of amyotrophic lateral sclerosis. The Journal of comparative neurology 490, 209-219.

Schnabel, J., 2008. Neuroscience: Standard model. Nature 454, 682-685.
Scott, S., Kranz, J.E., Cole, J., Lincecum, J.M., Thompson, K., Kelly, N., Bostrom, A., Theodoss, J., Al-Nakhala, B.M., Vieira, F.G., Ramasubbu, J., Heywood, J.A., 2008. Design, power, and interpretation of studies in the standard murine model of ALS. Amyotroph Lateral Scler 9, 4-15.

Tobina, T., Nakashima, H., Mori, S., Abe, M., Kumahara, H., Yoshimura, E., Nishida, Y., Kiyonaga, A., Shono, N., Tanaka, H., 2009. The utilization of a biopsy needle to obtain small muscle tissue specimens to analyze the gene and protein expression. The Journal of surgical research 154, 252-257.

Turner, B.J., Talbot, K., 2008. Transgenics, toxicity and therapeutics in rodent models of mutant SOD1-mediated familial ALS. Progress in neurobiology 85, 94-134.

Vande Velde, C., Garcia, M.L., Yin, X., Trapp, B.D., Cleveland, D.W., 2004. The neuroprotective factor Wlds does not attenuate mutant SOD1-mediated motor neuron disease. Neuromolecular medicine 5, 193-203.

Veldink, J.H., Bar, P.R., Joosten, E.A., Otten, M., Wokke, J.H., van den Berg, L.H., 2003. Sexual differences in onset of disease and response to exercise in a transgenic model of ALS. Neuromuscul Disord 13, 737-743.

Vincent, P., Maskos, U., Charvet, I., Bourgeais, L., Stoppini, L., Leresche, N.,
Changeux, J.P., Lambert, R., Meda, P., Paupardin-Tritsch, D., 2006. Live imaging of neural structure and function by fibred fluorescence microscopy. EMBO reports 7, 1154-1161.

Walsh, M.K., Lichtman, J.W., 2003. In vivo time-lapse imaging of synaptic takeover associated with naturally occurring synapse elimination. Neuron 37, 67-73.

Wang, M.S., Davis, A.A., Culver, D.G., Glass, J.D., 2002. WldS mice are resistant to paclitaxel (taxol) neuropathy. Annals of neurology 52, 442-447.

Wilbrey, A.L., Haley, J.E., Wishart, T.M., Conforti, L., Morreale, G., Beirowski, B., Babetto, E., Adalbert, R., Gillingwater, T.H., Smith, T., Wyllie, D.J., Ribchester, R.R., Coleman, M.P., 2008. VCP binding influences intracellular distribution of the slow Wallerian degeneration protein, Wld(S). Molecular and cellular neurosciences 38, 325-340.

Winlow, W., Usherwood, P.N., 1975. Ultrastructural studies of normal and degenerating mouse neuromuscular junctions. Journal of neurocytology 4, 377-394.

Wishart, T.M., Macdonald, S.H., Chen, P.E., Shipston, M.J., Coleman, M.P., Gillingwater, T.H., Ribchester, R.R., 2007a. Design of a novel quantitative PCR (QPCR)-based protocol for genotyping mice carrying the neuroprotective Wallerian degeneration slow (Wlds) gene. Molecular neurodegeneration 2, 21.

Wishart, T.M., Paterson, J.M., Short, D.M., Meredith, S., Robertson, K.A., Sutherland, C., Cousin, M.A., Dutia, M.B., Gillingwater, T.H., 2007b. Differential proteomics analysis of synaptic proteins identifies potential cellular targets and protein mediators of synaptic neuroprotection conferred by the slow Wallerian degeneration (Wlds) gene. Mol Cell Proteomics 6, 1318-1330.

Molecular and Cellular Neuroscience, Volume 42, Issue 4, November 2009, Pages 296–307
http://dx.doi.org/10.1016/j.mcn.2009.08.002

Table/ Figure Legends

Table 1

Inheritance test results of phenodeviants identified in the ENU-mutagensis/ CME screen.

One phenodeviant with enhanced axon degeneration and six phenodeviants with suppression of synaptic degeneration were identified in the screen. Inheritance test results from wild-type (+/+) mice were negative (0%) for all phenodeviants showing synaptic protection and Wld^S/+ inheritance test results of CEMOP_A1, CEMOP_S1, CEMOP_S4 and CEMOP_S6 were also negative (0%). Wld^S/+ inheritance test results of CEMOP_S2 was 12.5%, possibly due to a low penetrance mutation. Wld^S/+ inheritance test results of CEMOP_S3 and CEMOP_S5 were approximately 31% and 68% respectively suggesting Mendelian inheritance of a dominant mutation at least in the case of CEMOP_S5.

Molecular and Cellular Neuroscience, Volume 42, Issue 4, November 2009, Pages 296–307
http://dx.doi.org/10.1016/j.mcn.2009.08.002

Figure 1

Motor nerve terminals are not protected from Wallerian degeneration in *Wld*^{S} heterozygotes

Conventional confocal microscopic images of distal tibial nerve axons (A-C) and neuromuscular junctions in deep lumbrical muscles (DL; D-F) three days after ipsilateral section of the sciatic nerve. Axons and nerve terminals are labelled via transgenic expression of YFP. Postsynaptic acetylcholine receptors were labelled with TRITC–α–Bungarotoxin to visualise motor endplates. Axons and motor nerve terminals degenerate rapidly in wild-type (+/+; A,D). Axons are protected in *Wld*^{S} heterozygotes (B,E), which express about half the level of mutant protein compared with homozygotes, but motor nerve terminals are not. Both axons and nerve terminals are protected in *Wld*^{S} homozygotes (C,F). The time course of synaptic degeneration (G) was measured by scoring the percentage of all endplates in whole-mounts of DL muscles (about 250 fibers per muscle) that were 'vacant': that is, with no overlying YFP positive terminal (as in D,E). The rate of degeneration of nerve terminals in wild-type mice is not discernibly different from that in *Wld*^{S} heterozygotes and both are much more rapid than degeneration of motor nerve terminals in *Wld*^{S} homozygotes. Each point represents mean data from up to four lumbrical muscles from three to four mice (total number of axotomized lumbrical muscles examined D-33; E-56; F-29). Smooth curves shown are empirical fits to the data, for clarity only. Calibration bar: 50 μm.

Figure 2

CME resolved intact from degenerating axons or neuromuscular synapses

A. Low power view through a dissecting microscope of the Proflex 1.5 mm probe used to image the tibial nerve, exposed through a small skin incision, and the adjacent gastrocnemius muscle. B: intramuscular axons and motor nerve terminals in an innervated *thy1.2-YFP16* mouse gastrocnemius muscle with an intact sciatic nerve. C: Axons in the tibial nerve of *thy1.2-YFP16* mice all degenerated by 3 days after section of the sciatic nerve, in contrast to the extensive axonal protection seen in *Wld*^{S} mouse nerves. D: Axotomized tibial nerve axons are also preserved 3 days after sciatic nerve section in *thy1.2YFP16-Wld*^{S} heterozygotes, indistinguishable from wild-type and axotomised *Wld*^{S} homozygotes (data not shown). E. Intact NMJ's in the gastrocnemius muscle of a *Wld*^{S} homozygote were observable with CME 3 days after sciatic nerve injury but, F: no intact NMJ's were ever seen in *thy1.2-YFP/Wld*^{S} heterozygotes at this time point.

Molecular and Cellular Neuroscience, Volume 42, Issue 4, November 2009, Pages 296–307
http://dx.doi.org/10.1016/j.mcn.2009.08.002

Figure 3

Schematic representation of the CME driven ENU screen. *thy1.2-YFP16/Wld*^{S} double homozygous female mice on a C57BL/6 background were crossed to ENU-mutagenized BALB/c male mice. The sciatic nerves of the ENU-*Wld*^{S}/+ F1 offspring were transacted unilaterally under anaesthesia at 4-6 weeks of age. Following recovery 3 days later, the mice were reanaesthetized. The distal axons of the severed sciatic nerve were visualized in the tibial nerve via a small (< 5mm) incision in the skin, using a 1.5mm diameter fiber-optic probe connected to the CME computer. Superficial neuromuscular junctions were then visualized in the gastrocnemius muscle by manipulating the probe tip within the same cutaneous aperture. Mice showing deviation from the normal phenotype of *Wld*^{S}/+ mice: specifically those showing greater axonal degeneration (CEMOP_A) or stronger synaptic protection (CEMOP_S) than expected, were recovered from anaesthesia and subsequently transferred to breeding schedules to test for inheritance of the deviant phenotype.

Figure 4

Imaging with CME distinguishes intact from degenerating NMJ's and axons in *Wld*^{S} mice and ENU-phenodeviants. A-C Evidence of synaptic protection in three F1 ENU/ *thy1.2-YFP/Wld*^{S} crosses, 3 days after sciatic nerve section (CEMOP_S1, S2 and S5). All these phenodeviants were genetically heterozygous for *Wld*^{S}. These images were all obtained from sequences (movies) captured at 12 frames per second. Movies from phenodeviants CEMOP_S3 and CEMOP_S5 are shown in Supplementary Movies 3 & 4. D: Fragmented axons were observed 3 days after sciatic nerve section in the tibial nerve of ENU-mutant CEMOP_A1 that was heterozygous for *Wld*^{S}.

Figure 5

CME enables In vivo time-lapse imaging of synaptic degeneration at axotomised neuromuscular junctions in Wld^S mice

CME images of a group of neuromuscular junctions in a homozygous thy1.2-YFP16/Wld^S flexor digitorum longus muscle A) 3 days; B) 4 days; C) 5 days after section of the sciatic nerve. Arrows indicate neuromuscular junctions that degenerated over the two successive 24 hour periods.

Molecular and Cellular Neuroscience, Volume 42, Issue 4, November 2009, Pages 296–307
http://dx.doi.org/10.1016/j.mcn.2009.08.002

Figure 6

Imaging NMJ's with CME shows synapse loss in *thy1.2-YFP16/SOD1^{G93A}* mice. A, B : images of a group of gastrocnemius NMJ's obtained four days apart. Motor nerve terminals indicated by arrows in A had evidently degenerated by the time of the second viewing in B. These images were obtained from real-time movies obtained using CME (Supplementary Movies 2 & 3). Neuromuscular abnormalities including thinning of preterminal axons and degeneration of motor nerve terminals were also detected using this method (C, arrows). These features of neuromuscular pathology were also observed using conventional confocal microscopy, D: in a lumbrical muscles from the same mouse post-mortem; and E: in another SOD1 mouse sacrificied at end-stage of disease.

Figure 7

Slow axonal regeneration is also detected in ENU-mutant *ostes* using CME. A-C: The CME technique also proved effective in monitoring slow axonal regeneration in *thy1.2YFP-ostes* ENU mutant mice. A: wild-type mouse tibial nerve, 10 days after crush injury of the sciatic nerve. Extensive axon regeneration is evident by presence of intact axons. B: discernibly fewer axons regenerated in *ostes* heterozygotes at the same time point indicating a slower rate of regeneration. C: In *ostes* homozygotes continuous axons were not observed in the tibial nerve 10 days after sciatic crush, only autofluorescence in the vicinity of the degenerated axons could be seen, indicating even slower regeneration. D-F: corresponding images from the tibial nerves of the same mice obtained by conventional confocal microscopic post mortem: G-H: Conventional confocal microscopy of neuromuscular junctions in lumbrical muscles of wild-type (G), *ostes*/+ (H) and *ostes/ostes* (I) mice 20 days after sciatic nerve crush. NMJ's were fully reinnervated in wild-type (G) mice, whereas there is only partially reinnervation in *ostes*/+ (H) mice shown by the presence of some vacant endplates. NMJ's in *ostes/ostes* mice were completely vacant and therefore not reinnervated (I).

Molecular and Cellular Neuroscience, Volume 42, Issue 4, November 2009, Pages 296–307
http://dx.doi.org/10.1016/j.mcn.2009.08.002

Supplementary Figures:

Supplementary Figure S1

Synaptic protection in CEMOP_S5 is inherited. The CEMOP_S5 founder, heterozygous for *thy1.2-YFP:16* and *Wld*^{S}, was crossed to a C57BL6 control mouse that was homozygous for thy1.2-YFP:16. The twelve mice obtained in the first litter shown were genotyped for the *Wld*^{S} allele by real-time PCR. Still images captured from sequences using CME are shown for the mice with its litter identification code on the top left of each image. The image sequence from mouse 1.1j is shown in Supplementary Movie 5. All the wild-type mice show fragmented nerve endings, but four out of seven heterozygous *Wld*^{S} mice show protected intramuscular collaterals and motor nerve terminals (arrows). Mouse 1.1a was sacrificed and the lumbrical muscles were dissected and the conventional confocal image (colour image, upper right) confirmed the strong synaptic protection observed using CME.

Supplementary Figure S2

Visualization of NMJ's axons and in SOD1^{G93A} mice using CME

A: Intact NMJ's visualized by CME in a control, SOD1^{G93A}-negative littermate of the mouse shown in Supplementary Movie 6 (and NMJ's in Figure 6A-C). B: Evidence of axonal sprouting (arrow) visualized by CME in a SOD1^{G93A} symptomatic mouse. C: Intact tibial nerve axons visualized by CME in the SOD1^{G93A} mouse shown in Supplementary Movie 6 (gastrocnemius NMJ's shown in Figure 6A). D: Intact tibial nerve axons visualized by CME in the SOD1^{G93A} mouse shown in Supplementary Movie 6 (gastrocnemius NMJ's shown in Figure 6B), obtained four days after the image shown in C. There is no evidence of axonal degeneration suggesting the initial visualization did not cause photodamage to the YFP-fluorescent axons.

Supplementary Figure S3

Axonal regeneration and reinnervation of NMJs in *Ostes* mice.

Axons were fully regenerated in wild-type (A) and *ostes*/+ (B) mice 20 days after sciatic nerve crush, however axons in *ostes/ostes* (C) were less dense, indicating a slower rate of regeneration. At 30 day post-crush, axons have fully regenerated in wild-type (D), *ostes*/+ (E) and *ostes/ostes* (F) mice. There was no discernible difference between the axons of these mice (D-F).

Molecular and Cellular Neuroscience, Volume 42, Issue 4, November 2009, Pages 296–307
http://dx.doi.org/10.1016/j.mcn.2009.08.002

Supplementary Movies

Supplementary Movie 1: Real-time images obtained by CME showing intact intramuscular axons and neuromuscular junctions in a control, unoperated *thy1.2-YFP16* mouse. One of the frames from this movie is shown in Figure 3A.

Supplementary Movie 2: Real-time images obtained by CME showing intact intramuscular axons and neuromuscular junctions in the gastrocnemius muscle of a *thy1.2-YFP16/Wld^S* homozygote, 3 days after section of the sciatic nerve. One of the frames from this movie is shown in Figure 3B.

Supplementary Movie 3: Real-time images obtained by CME showing intact intramuscular axons and neuromuscular junctions in the gastrocnemius muscle of an ENU-mutant *thy1.2-YFP16/Wld^S* heterozygote, 3 days after section of the sciatic nerve. This mouse was designated CEMOP_S2 and showed strong deviation (synaptic protection) compared with the normal *Wld^S*/+ phenotype. One of the frames from this movie is shown in Figure 3E.

Supplementary Movie 4: Real-time images obtained by CME showing intact intramuscular axons and neuromuscular junctions in the gastrocnemius muscle of an ENU-mutant *thy1.2-YFP16/Wld^S* heterozygote, 3 days after section of the sciatic nerve. This mouse was designated CEMOP_S5 and showed strong deviation (synaptic protection) compared with the normal *Wld^S*/+ phenotype. One of the frames from this movie is shown in Figure 3F.

Supplementary Movie 5: Real-time images obtained by CME showing intact intramuscular axons and neuromuscular junctions in the axotomized muscle of the F1-offspring 1.1j from ENU-mutant CEMOP_S5 (See Figure 4). The gastrocnemius NMJ's in this *thy1.2-YFP16/Wld^S* heterozygote were examined 3 days after section of the sciatic nerve. One of the frames from this movie is shown in Figure 4.

Supplementary Movie 6: The 8-month old, liminally-symptomatic *thy1.2-YFP/SOD1^{G93A}* mouse from which images of NMJ's shown in Figure 1 were subsequently obtained. The mouse only showed signs of abnormal gait, including splaying of the hind feet, before imaging with CME (Supplementary Movies 7,8).

Supplementary Movie 7: Real-time images obtained by CME in the gastrocnemius muscle of the mouse shown in Supplementary Movie 6. One of the frames from this

Molecular and Cellular Neuroscience, Volume 42, Issue 4, November 2009, Pages 296–307
http://dx.doi.org/10.1016/j.mcn.2009.08.002

movie is shown in Figure 6A.

Supplementary Movie 8: Real-time images obtained by CME in the gastrocnemius muscle of the mouse shown in Supplementary Movie 6, four days after obtaining the movie shown in Supplementary Movie 7. One of the frames from this movie is shown in Figure 6B.

Molecular and Cellular Neuroscience, Volume 42, Issue 4, November 2009, Pages 296–307
http://dx.doi.org/10.1016/j.mcn.2009.08.002

Name of Phenodeviant	Modification of Wld^S/+ Phenotype	Inheritance Test Results (+/+)	Inheritance Test Results (Wld^S/+)
CEMOP_A1	Axon degeneration	N/A	0/21 (0%)
CEMOP_S1	Synaptic protection	0/10 (0%)	0/15 (0%)
CEMOP_S2	Synaptic protection	0/21 (0%)	2/16 (12.5%)
CEMOP_S3	Synaptic protection	0/14 (0%)	5/16 (31.3%)
CEMOP_S4	Synaptic protection	0/19 (0%)	0/17 (0%)
CEMOP_S5	Synaptic protection	0/24 (0%)	17/25 (68%)
CEMOP_S6	Synaptic protection	0/7 (0%)	0/14 (0%)

Table 1

Inheritance test results of phenodeviants identified in the ENU-mutagensis/ CME screen.

One phenodeviant with enhanced axon degeneration and six phenodeviants with suppression of synaptic degeneration were identified in the screen. Inheritance test results from wild-type (+/+) mice were negative (0%) for all phenodeviants showing synaptic protection and Wld^S/+ inheritance test results of CEMOP_A1, CEMOP_S1, CEMOP_S4 and CEMOP_S6 were also negative (0%). Wld^S/+ inheritance test results of CEMOP_S2 was 12.5% suggesting a low penetrance mutation. Wld^S/+ inheritance test results of CEMOP_S3 and CEMOP_S5 were approximately 31% and 68% respectively suggesting Mendelian inheritance of a dominant mutation at least in the case of CEMOP_S5.

Molecular and Cellular Neuroscience, Volume 42, Issue 4, November 2009, Pages 296–307
http://dx.doi.org/10.1016/j.mcn.2009.08.002

Figure 1

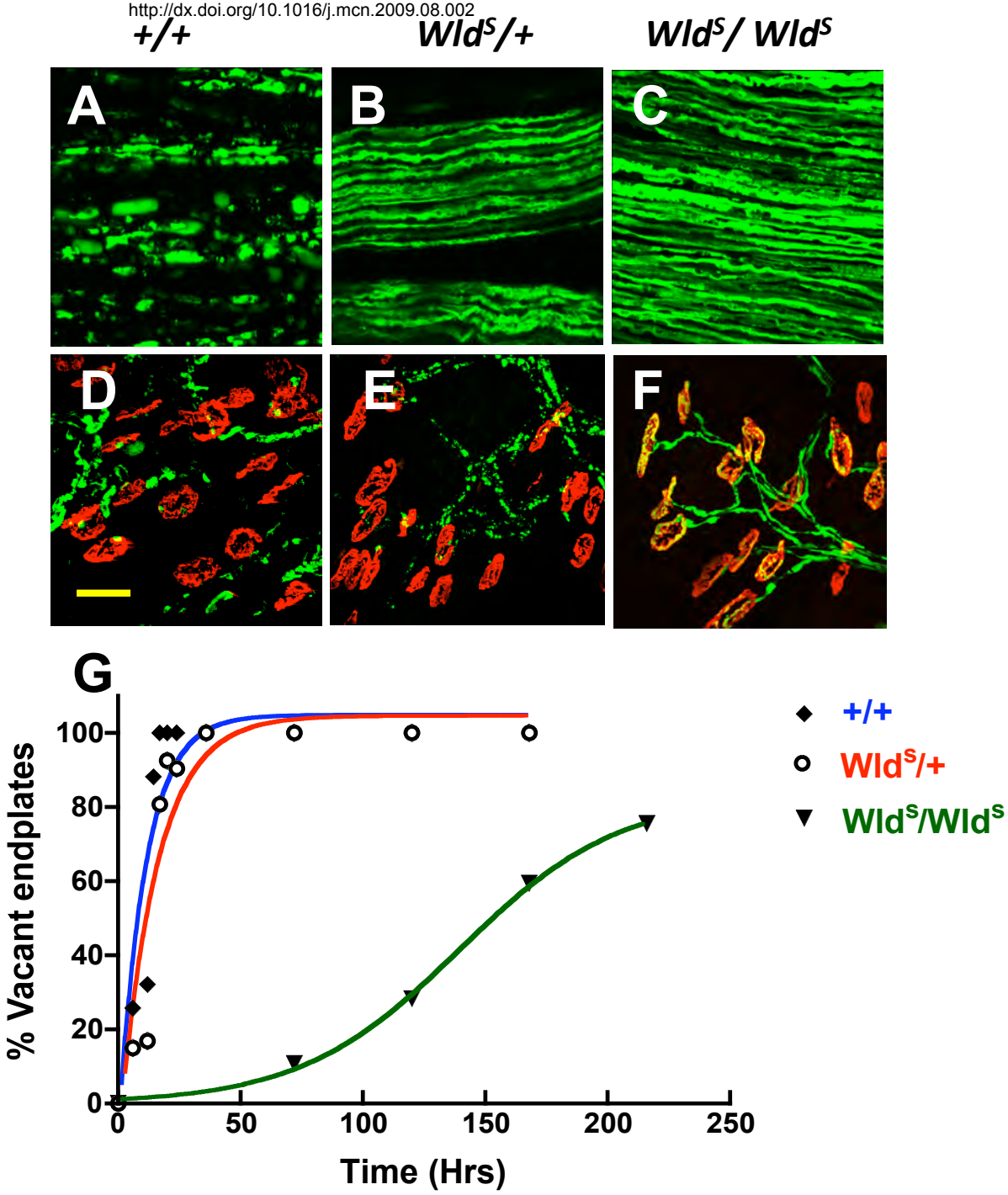

Molecular and Cellular Neuroscience, Volume 42, Issue 4, November 2009, Pages 296–307
http://dx.doi.org/10.1016/j.mcn.2009.08.002

Figure 2

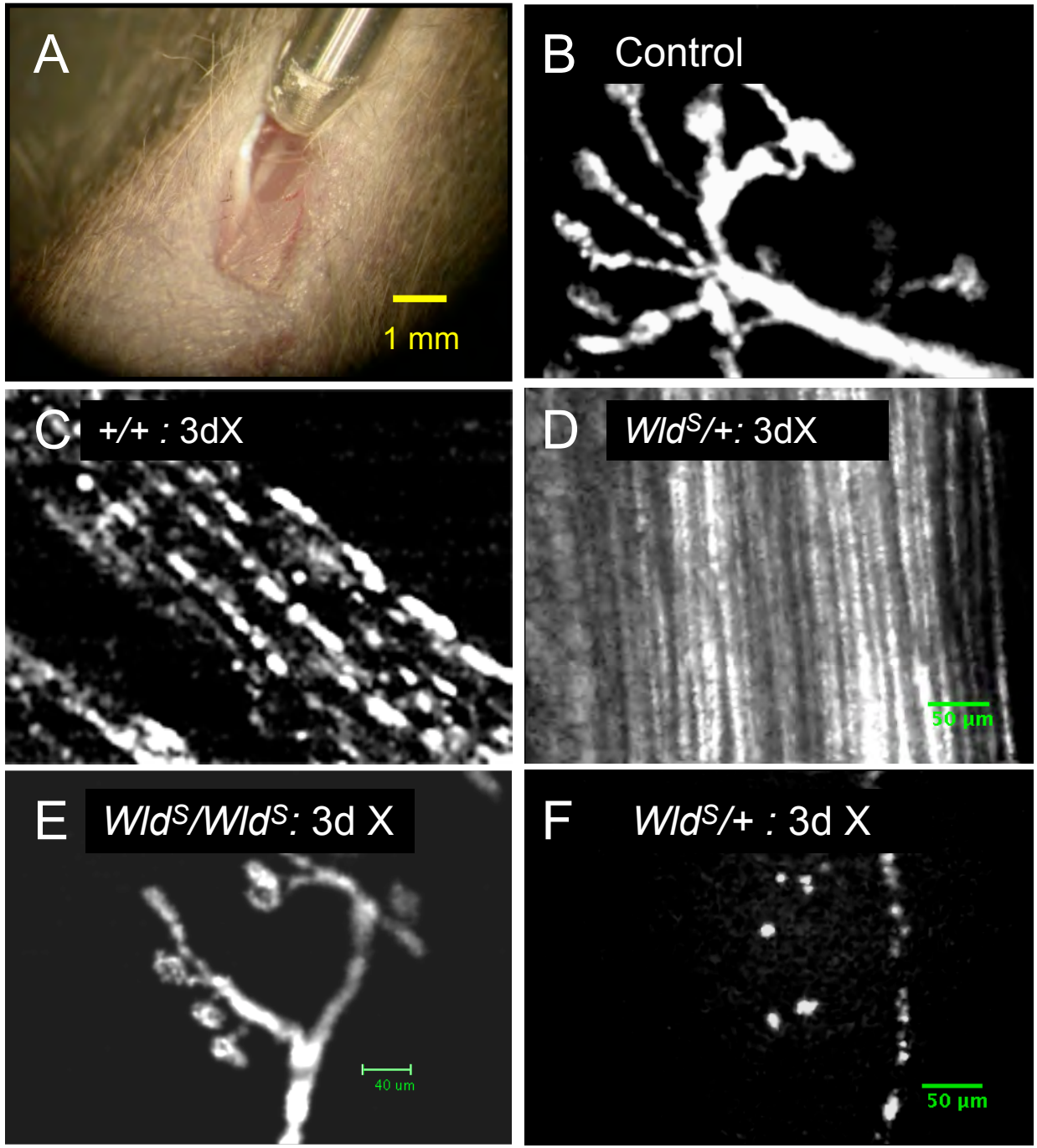

Molecular and Cellular Neuroscience, Volume 42, Issue 4, November 2009, Pages 296–307
http://dx.doi.org/10.1016/j.mcn.2009.08.002

Figure 3

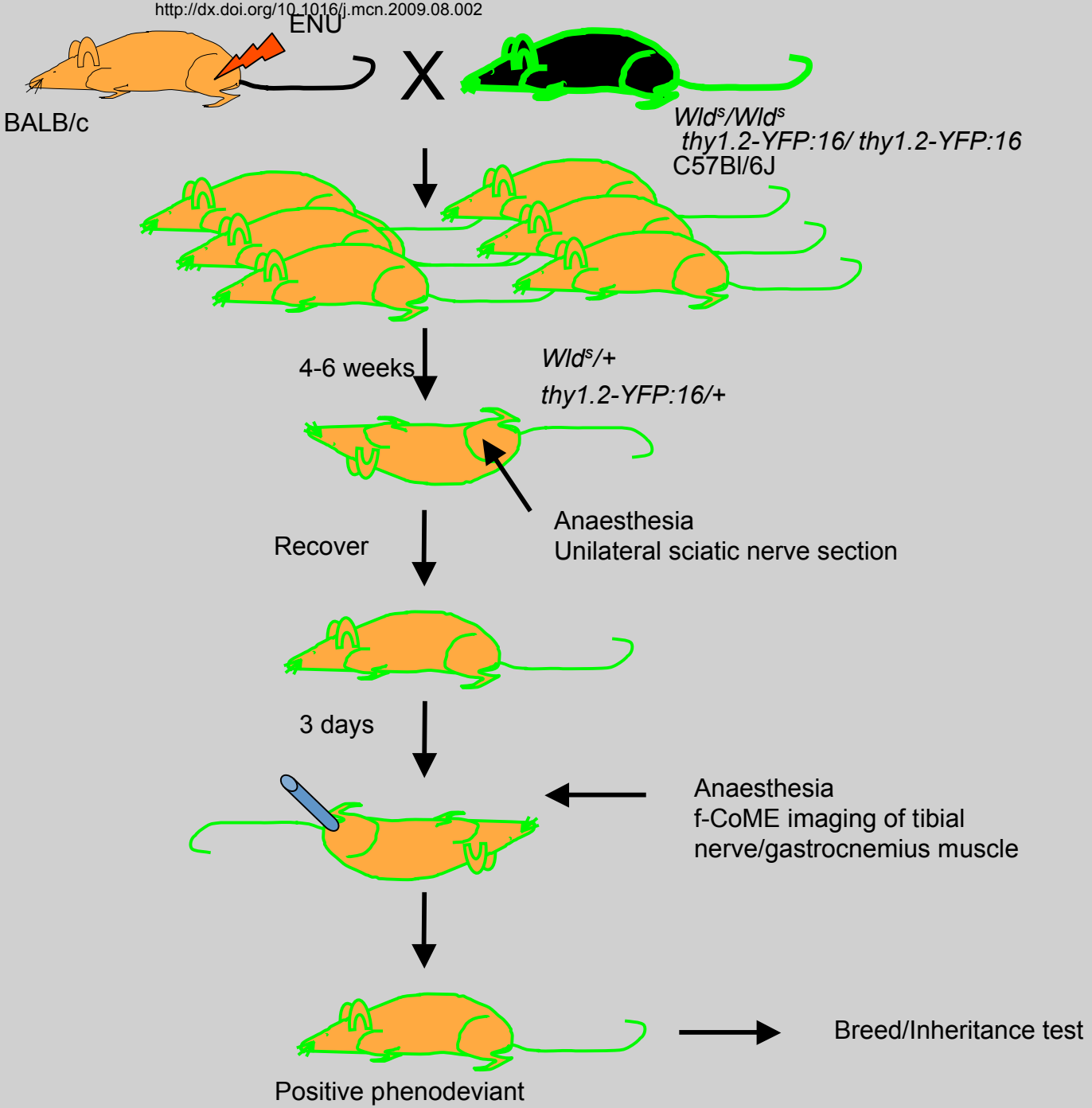

Molecular and Cellular Neuroscience, Volume 42, Issue 4, November 2009, Pages 296–307
http://dx.doi.org/10.1016/j.mcn.2009.08.002

Figure 4

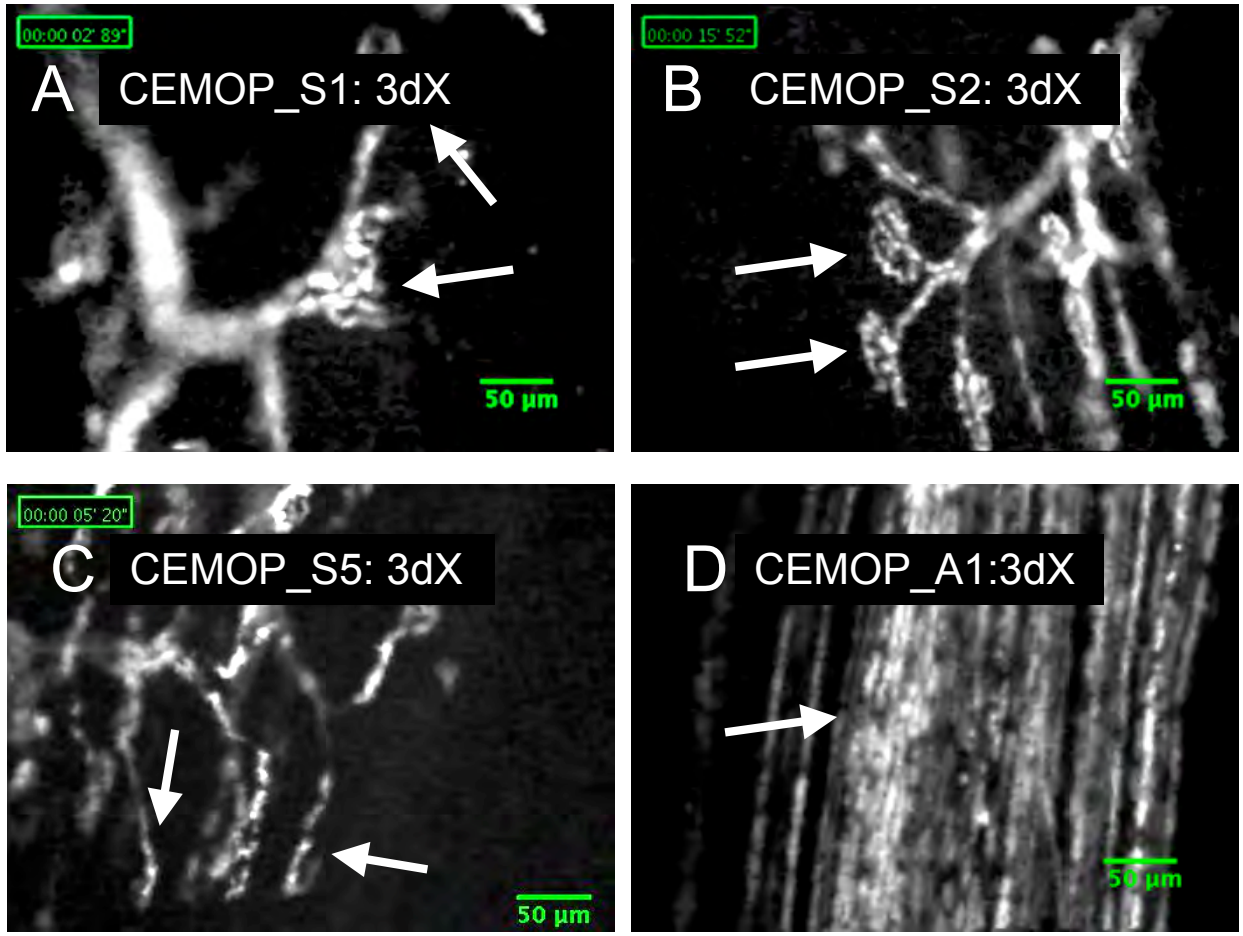

Molecular and Cellular Neuroscience, Volume 42, Issue 4, November 2009, Pages 296–307
http://dx.doi.org/10.1016/j.mcn.2009.08.002

Figure 5

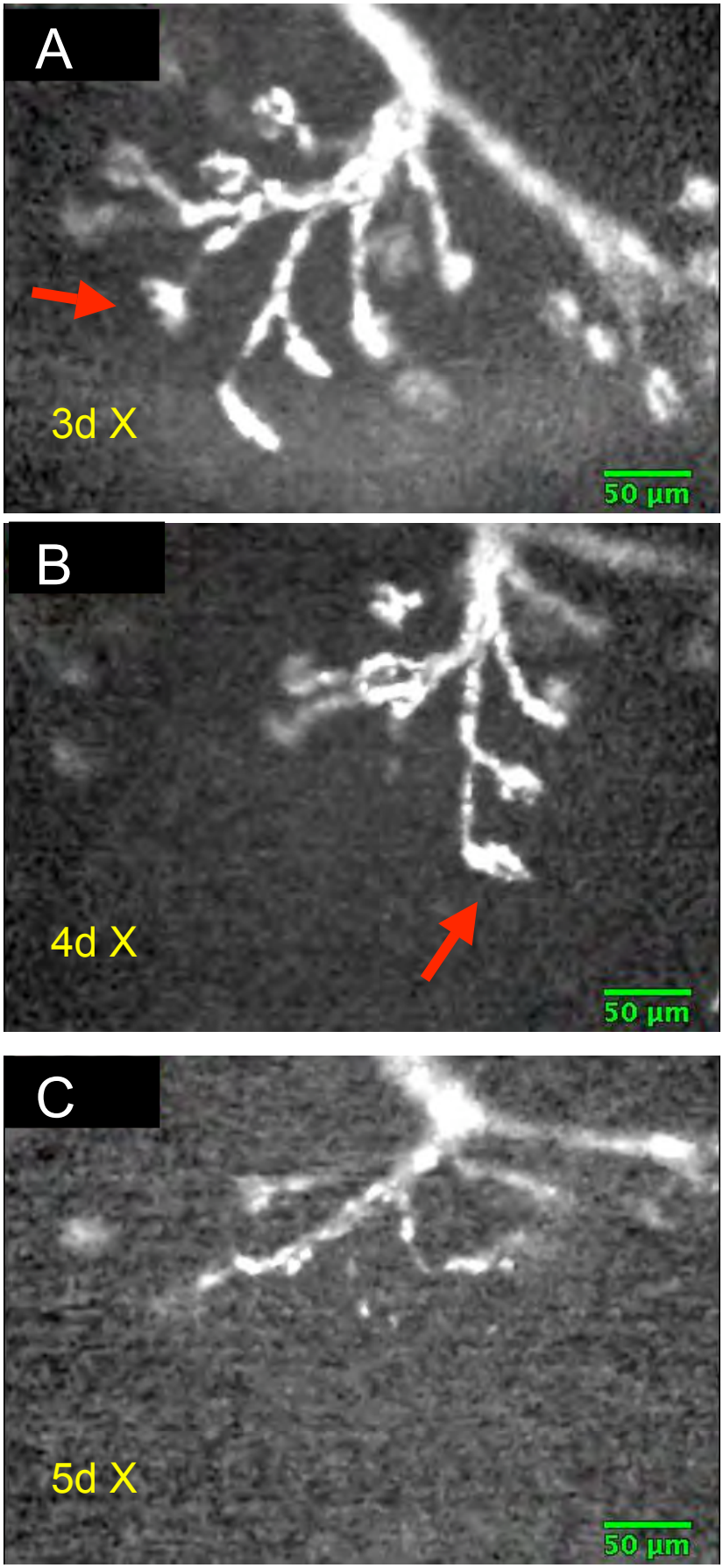

Molecular and Cellular Neuroscience, Volume 42, Issue 4, November 2009, Pages 296–307
http://dx.doi.org/10.1016/j.mcn.2009.08.002

Figure 6

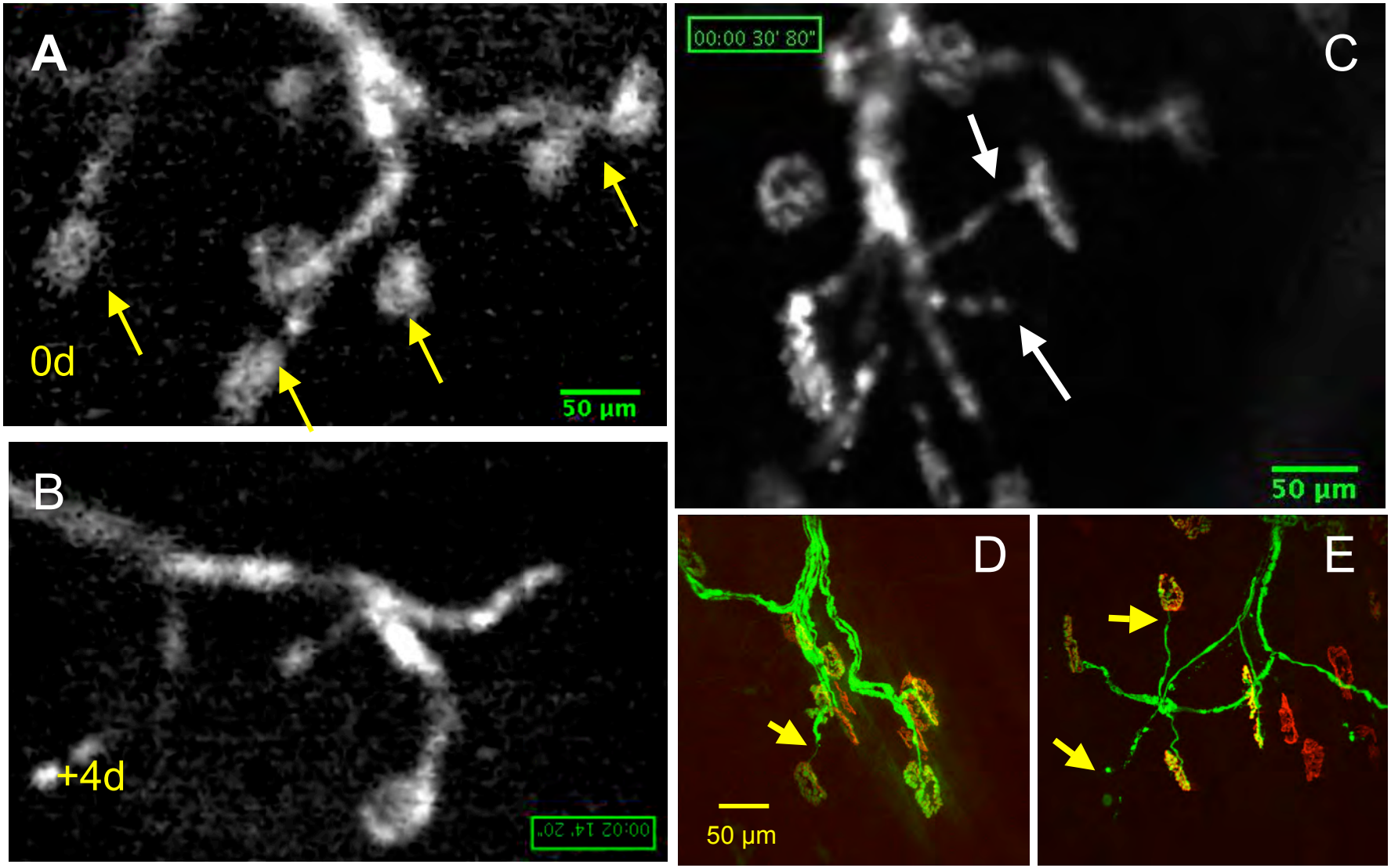

Molecular and Cellular Neuroscience, Volume 42, Issue 4, November 2009, Pages 296–307
http://dx.doi.org/10.1016/j.mcn.2009.08.002

Figure 7

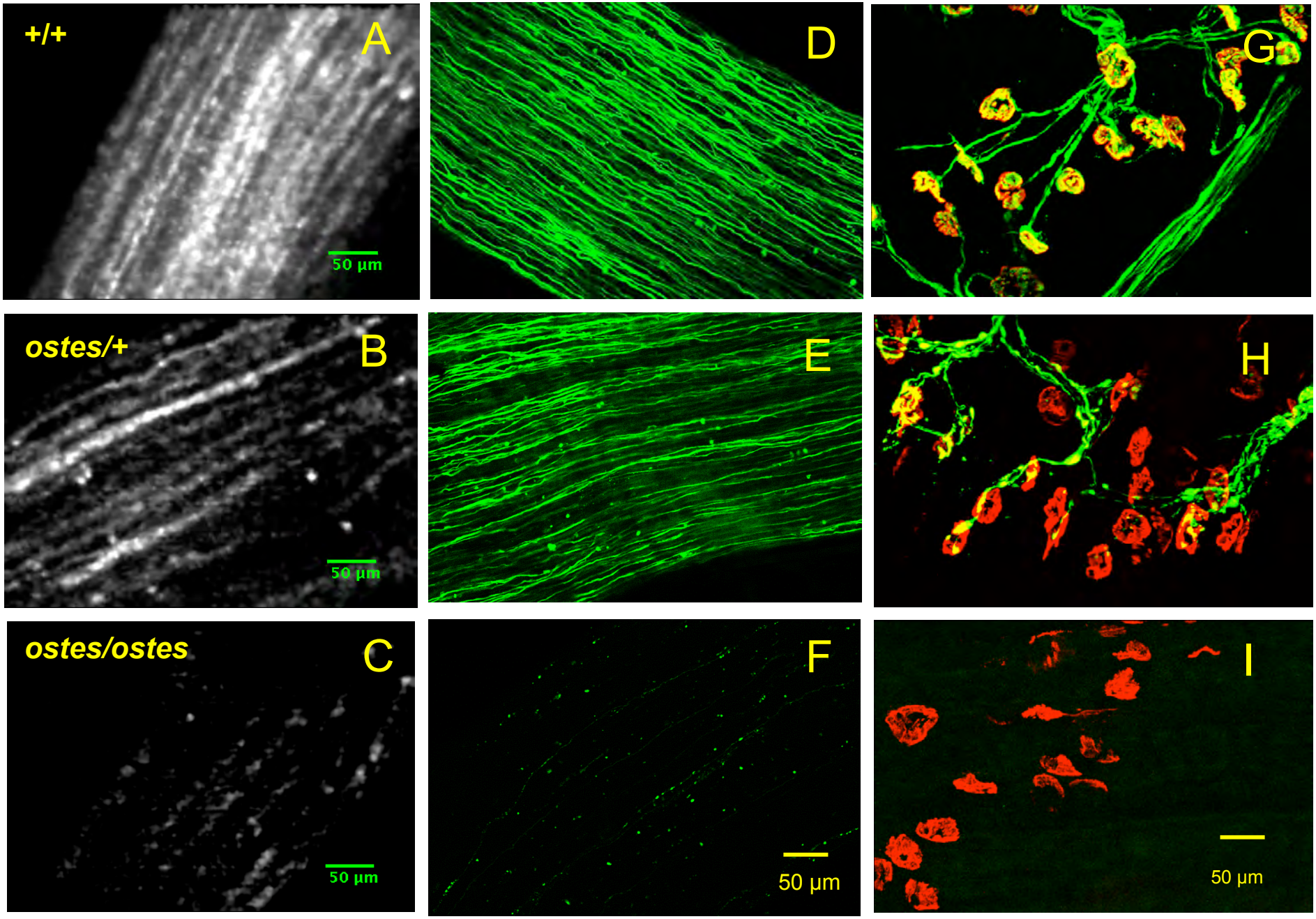

Molecular and Cellular Neuroscience, Volume 42, Issue 4, November 2009, Pages 296–307
http://dx.doi.org/10.1016/j.mcn.2009.08.002

Supplementary Figure S1

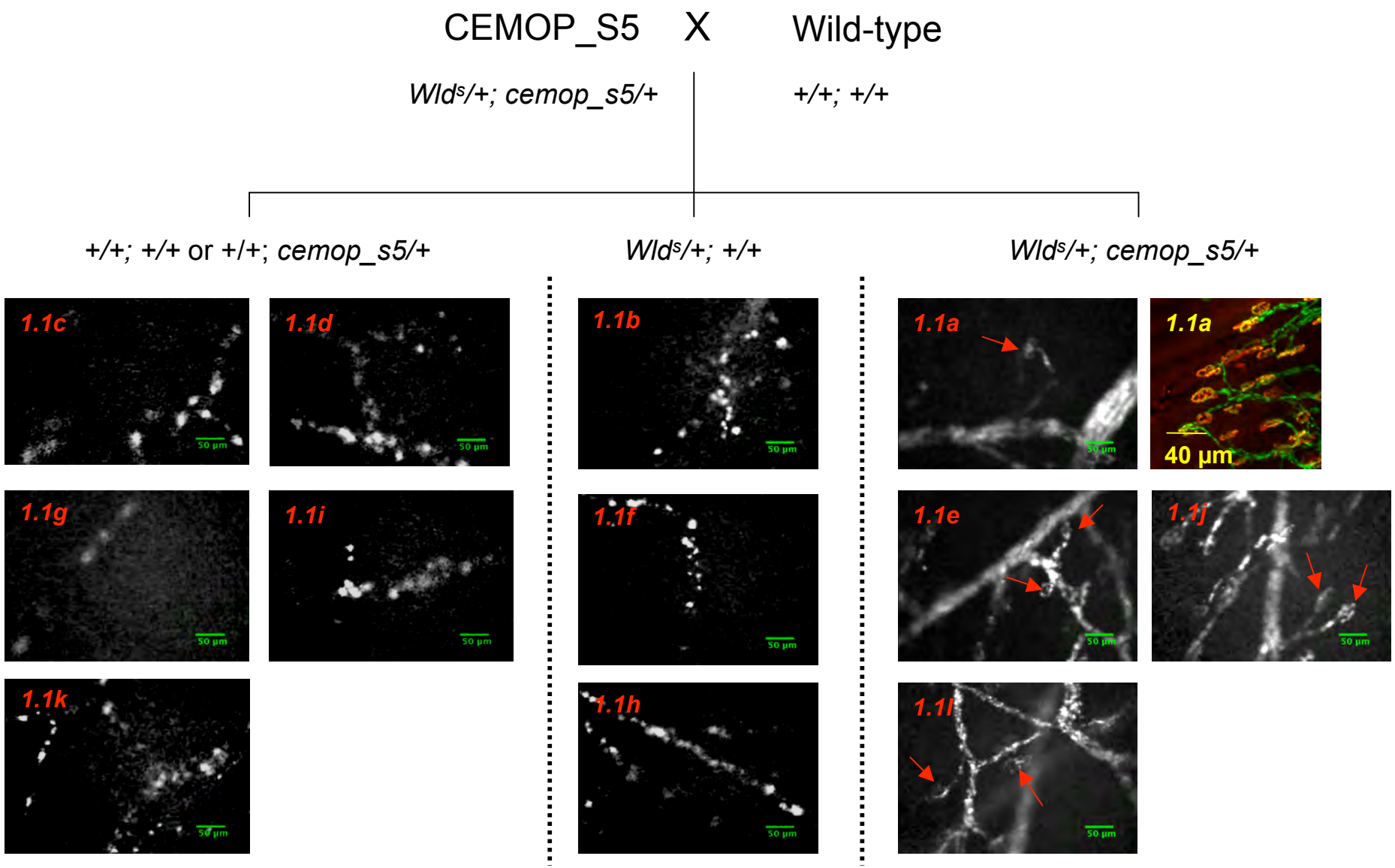

Molecular and Cellular Neuroscience, Volume 42, Issue 4, November 2009, Pages 296–307
http://dx.doi.org/10.1016/j.mcn.2009.08.002

Supplementary Figure S2

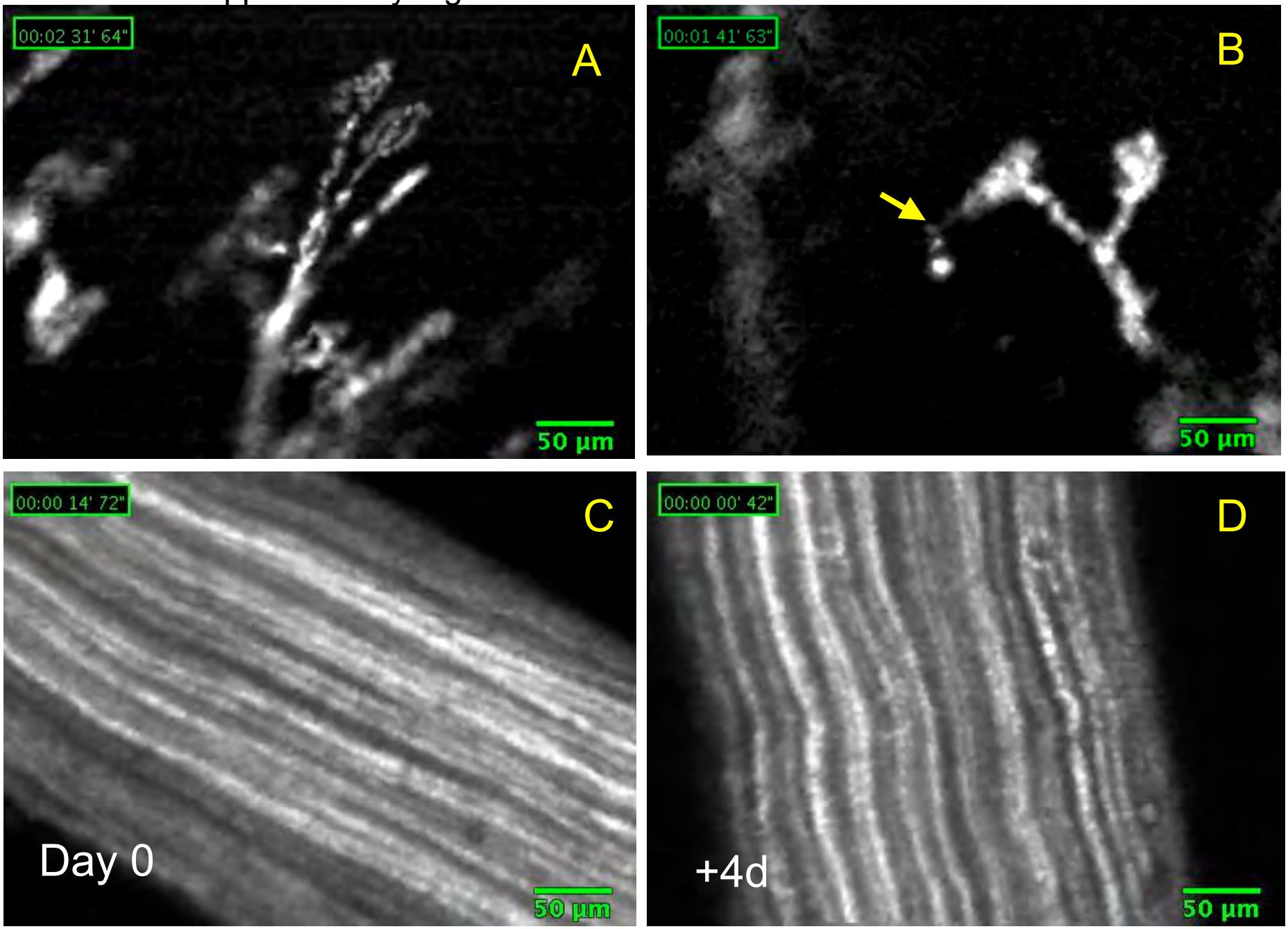

Molecular and Cellular Neuroscience, Volume 42, Issue 4, November 2009, Pages 296–307
http://dx.doi.org/10.1016/j.mcn.2009.08.002

Supplementary Figure S3